DEVELOPMENT OF AUTOMATIC LOAD-SHEDDING STRATEGY

FOR STAND-ALONE PHOTOVOLTAIC SYSTEM

MASHITAH BINTI MOHD FARITH

Bachelor of Electrical Engineering

(Power Electronic And Drives)

June 2014

" I hereby declare that I have read through this report entitle "Development Of Automatic Load-Shedding Strategy For Stand-Alone Photovoltaic System" and found that it has comply the partial fulfillment for awarding the degree of Bachelor of Electrical Engineering (Power Electronic and Drive) "

Signature   : ………………………….

Supervisor's Name   : Mr. Mohamad Na'im bin Mohd Nasir

Date   : ………………………….

DEVELOPMENT OF AUTOMATIC LOAD-SHEDDING STRATEGY FOR STAND-ALONE PHOTOVOLTAIC SYSTEM

MASHITAH BINTI MOHD FARITH

**A report submitted in partial fulfillment of the requirement for the degree
of Bachelor in Electrical Engineering
(Power Electronic and Drive)**

**Faculty of Electrical Engineering
UNIVERSITI TEKNIKAL MALAYSIA MELAKA**

2013/2014

I declare that this report entitle "Development Of Automatic Load-Shedding Strategy For Stand-Alone Photovoltaic System" is the result of my own research except as cited I the reference. The report has not been accepted for any degree and is not concurrently submitted in candidature of any other degree.

Signature   : …………………………….
Name   : Miss Mashitah Binti Mohd Farith
Date   : …………………………….

ACKNOWLEDGEMENT

Alhamdulillah, many thanks to Allah, with His permission I complete my PSM2 successfully. Thanks to Allah for blessing me and for ease my way to complete this report. I would like to express the deepest appreciation to my supervisor, Mr. Mohamad Na'im bin Mohd Nasir for guiding, supervising and advising me along the completion of this report.

I would like to express my deepest gratitude to both my beloved father and mother who raised me well with loves and support. Thank you for giving me support, advise and also money to complete this report. One day, your kindness will be repay.

Last but not least, thank you to all my friend for giving me important information in completing the report. The supports from all of you are so unforgettable. Great thanks to all.

ABSTRACT

Nowadays, the use of solar energy are extremely developed and delivered worldwide. This project presents the development of automatic load-shedding strategy for stand-alone photovoltaic system. The design of this project shows the characteristics of solar energy and operation of load-shedding strategy. The main objective of this project is to implement the load-shedding strategy as an emergency controller for stand-alone photovoltaic system. To achieve the objective, research of basic understanding related to this project is very important to understand more about the characteristics of each element in this project. The circuit of the load-shedding system is designed in the SoftCad Eagle PCB Design software. The algorithm controlling the load-shedding scheme is developed in the Arduino IDE. Then, the coding programmed is burn in the microcontroller board and installed with the hardware. Output of this project can support the DC loads and load-shedding strategy scheme is performed based on the designed algorithm.

ABSTRAK

Pada masa kini, penggunaan tenaga solar adalah sangat maju dan tersebar di seluruh dunia. Projek ini membentangkan pembangunan strategi catuan beban secara automatik untuk sistem photovoltaic bersendirian. Reka bentuk projek ini menunjukkan ciri-ciri tenaga solar dan operasi strategi catuan beban. Objektif utama projek ini adalah untuk melaksanakan strategi catuan beban sebagai pengawal kecemasan untuk sistem photovoltaic bersendirian. Untuk mencapai matlamat tersebut , penyelidikan pemahaman asas yang berkaitan dengan projek ini adalah sangat penting untuk memahami lebih lanjut mengenai ciri-ciri bagi setiap elemen dalam projek ini. Litar sistem catuan beban telah direka dalam perisian SoftCad Eagle PCB Design. Algoritma mengawal skim catuan itu diprogramkan dalam perisian IDE Arduino . Kemudian, pengekodan yang diprogramkan telah dimuat turun ke dalam papan pengawal mikro dan dipasang dengan perkakasan. Pengeluaran projek ini boleh menyokong beban DC dan skim strategi catuan beban dilakukan berdasarkan algoritma yang direka.

TABLE OF CONTENT

LIST OF TABLES

LIST OF FIGURES

LIST OF ABBREVIATIONS

PV	-	Photovoltaic
PCB	-	Printed Circuit Board
DC	-	Direct Current
AC	-	Alternating Current
Si	-	Silicon
V	-	Volt
A	-	Ampere
W	-	Watt
MOSFET	-	Metal Oxide Semiconductor Field-Effect Transistor
LED	-	Light Emitting Diode
SRAM	-	Static Random Access Memory
EEPROM	-	Electrically Eraseable Programmable Read-Only Memory
I_{SENSE}	-	Sensed Current
V_{SENSE}	-	Sensed Voltage
V_{in}	-	Input Voltage
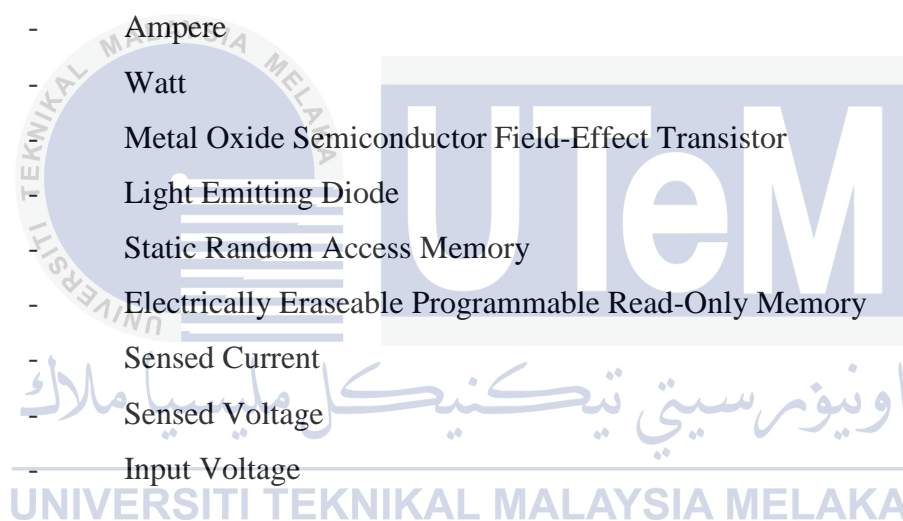
LIST OF APPENDICES

CHAPTER 1

INTRODUCTION

1.1   Project Background

The level of demand for electricity is very high as it is human necessities of life either during day time or night. Most of human daily routines such as work, economy, livelihood, healthcare and leisure depend on a constant power supply. Thus, even a temporary power failure can cause chaos, financial loss, and possible loss of life. There are several unexpected causes of power failure such as natural causes like weather, short circuit, components broken and others. However, in this modern day life, a lot of precaution steps are designed and implemented on the grid system to overcome the power failure. The islanded microgrid operation is one of the methods to keep certain places to receive power supply. This operation is supported by load-shedding scheduling which keeping the power system stability by turn off some of the loads. For this project, the application of load-shedding strategy for islanded microgrid system during power outages is implemented in a small scope where photovoltaic (PV) technology is used as a power supply. PV systems are low maintenance, provide a cleaner, environmentally friendly alternative, and very reliable source of power. It is often used as a back-up for the grid system or operates independently without grid connection. Successful stand-alone systems generally take advantage of a combination of techniques and technologies to generate reliable power, reduce costs, and minimize

in convenience. Therefore, this stand-alone PV system will supply several loads and to keep the system balance, load-shedding strategy will be implemented in this system.

1.2 Problem Statement

As the demand of electricity has increase throughout the decade, the failure of power system will affect the daily routines. Therefore, the methods to overcome power outages are developed and delivered worldwide such as the usage of solar energy, wind energy and biofuels energy as a back-up system. However, another issue has come out, there is a rising interest on their impacts on power system operation and control as they have low reliability and flexibility. For this project, a PV stand-alone system is installed to supply several loads. At a certain time, power generated by the PV might be low than the power consumed by the loads due to the variation of irradiances level. At this moment, the power consumed by the loads will not be at rated value and make the power demand higher than power supply. Therefore, the load-shedding strategy is applied to the system to give the maximum power to the loads. The algorithms for the load-shedding will be determined based on the load demand and acceptable power range from PV. The number of load to be shed is important to ensure the stability of energy conservation.

1.3 Objectives

The aims of this project are as follow:

1. To design automatic load-shedding strategy for stand-alone photovoltaic system.
2. To develop the algorithms to control the load-shedding operation.
3. To study the energy conservation between load and supply under variation of conditions.

1.4 Scope of Research

This project primarily focuses on three parts; which are the type of PV system, the strategy for load-shedding and type of load. In this project, the system designed is stand-alone PV system without connection of energy storage. Other than this type of PV system is not included in this project. This project performs only on the implementation of hardware. The circuit of hardware is designed by using SoftCad Eagle PCB Design software while the programming is developed by using Arduino IDE. The algorithms developed for load-shedding will be determined based on the load demand and the acceptable power range from PV. Furthermore, this project use number of lighting as a DC loads. This project will not cover the AC loads. This project is implemented as a prototype of load-shedding strategy for islanded microgrid operation during power outages in a small scope. Only operations during islanded microgrid operation after power failure is covered.
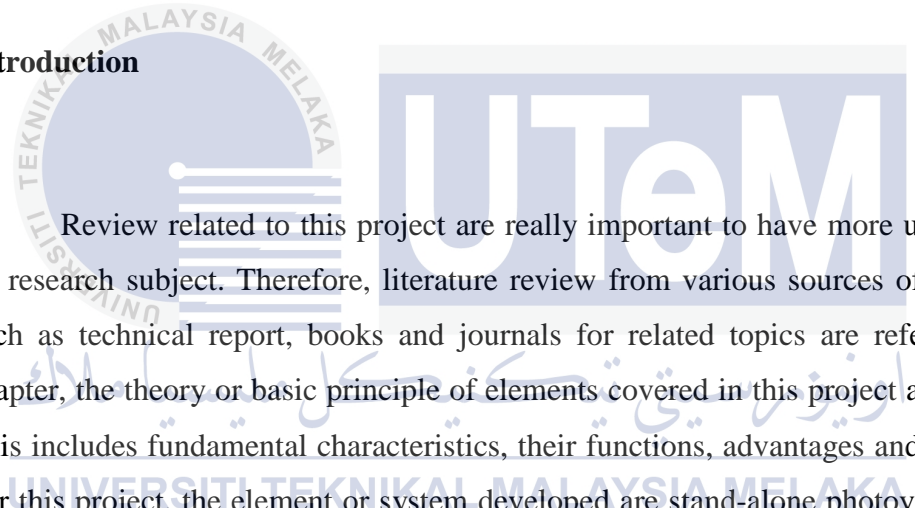
1.5 Report Outlines

1. **Chapter 1** - An introductory of the project consisting of the project problem statement, objectives, and scope.

2. **Chapter 2** – Collection of theories that can be formulated and implemented in the project. Reviews of literatures from various sources that can be related to the project research and development.

3. **Chapter 3** – Description of design methodology for the project development and progress.

4. **Chapter 4** – Results of the project progress is described and the analysis of the results are discussed.

5. **Chapter 5** – The conclusion and recommendation on the final stages of the project development.

CHAPTER 2

LITERATURE REVIEW

2.1   Introduction

Review related to this project are really important to have more understanding on research subject. Therefore, literature review from various sources of information such as technical report, books and journals for related topics are referred. In this chapter, the theory or basic principle of elements covered in this project are discussed. This includes fundamental characteristics, their functions, advantages and many more. For this project, the element or system developed are stand-alone photovoltaic system and load-shedding strategy.

2.2   Photovoltaic System

2.2.1   Definition

Genuinely, PV entail the process regarding the conversion of the radiant energy from the sun (solar energy) directly into the electricity [1]. Since the solar energy is the most abundant energy source on the planet, photovoltaic system can be classified as a vital technology that needs to be explored extensively in order to preserve our planet. PV sources can provide power supply to from the small electronics to homes and large commercial businesses. PV systems consist of various type of configuration such as grid connected PV system, direct PV system, stand-alone PV system and hybrid system [2].

2.2.2 Configurations

A PV cell is normally consists of a semiconductor diode whose p-n junction is exposed to light. Nowadays, most of PV which are more than 90% of them, are manufactured from Si modules constructed from small 4-12 inch crystalline or multicrystalline wafers [3]. Basically photovoltaic cell is made from several types of semiconductor such as monocrystalline and polycrystalline silicon cells. Silicon PV cells are composed of a thin layer of bulk Si or a thin Si film connected to electric terminals. One of the sides of the Si layer is doped to form p-n junction. A thin metallic grid is placed on the Sun-facing surface of the semiconductor [4].

The traditional Si solar cell is a homo junction device. It might have a p-type base with an acceptor (typically boron or aluminum) and a diffused n-type window/emitter layer (typically phosphorus). The Fermi level of the n-type side will be near the conduction (valence) band edge so that donor-released electrons will diffuse into the p-type side to occupy lower energy states there, until the exposed space charge (ionized donors in the n-type region, and ionized acceptors in the p-type) produces a field large enough to prevent further diffusion. To produce a back surface field (BSF)

for hole collection and rejects the electrons, a very heavily doped region is used at the back contact. Figure 2.1 indicates the typical construction of the semiconductor part of a Si cell.
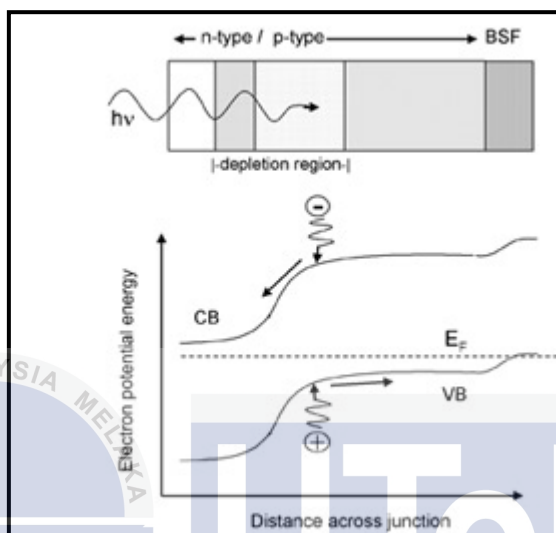
Figure 2.1: The Diagram Of Solar Cell Structure And Energy Band [3]

Most of the PV panels are covered with an aluminum frame around the edge, with the size about 600 mm wide, 1200 mm tall and 25 mm thick. These panels are combined together to form a PV array. The crytalline-type panel are the most efficient which operates at about 25% efficiency by maintaining the cool temperature. These type of panels are created from crystalline silicon cells which covered by a grid of wire to aid the electrical energy flow to the terminals. Besides that, there are cheaper PV panels compare to crystalline panels called thin film technologies panels. Material like amorphous silicon can be applied as a film without the need for a glass covering such as glass or plastic. However, the efficiency of thin film technologies panel is about 10% which is much lower than crystalline [5].

Some of PV systems need an inverter and batteries as one of the equipments, depend on the system requirement. The inverters are used to convert the DC value of

PV panels to AC value for AC system. The batteries are mostly needed for stand-alone PV systems which the place is not provided with connection to the electricity grid. These batteries keep the electrical power as a back-up when the PV panels cannot manage to supply adequate electricity. The grid connected systems need a metering system to calculate the amounts of electricity comes from the grid and also from the PV.

2.2.3 Operation

PV generates electricity by converting it directly from solar radiation through an electronic process that occurs in certain types of material called semiconductor. Solar energy release the electrons in these materials and can be induced to travel through an electric circuit which then powering electronic devices or supply electricity to the grid [6].
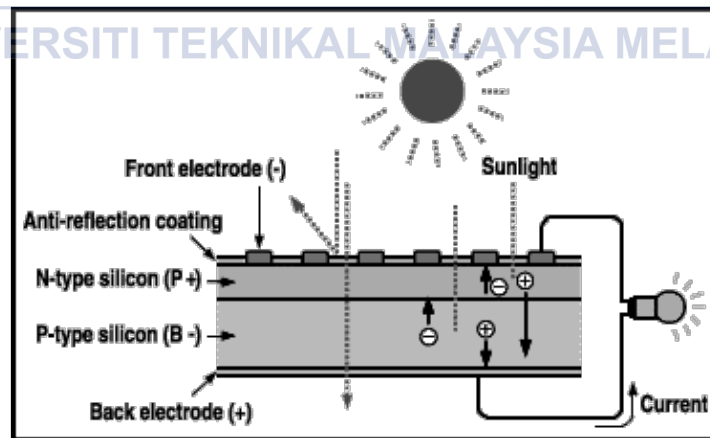

Figure 2.2: Basic Construction Of PV Systems [8]

The photons energy from the sun strike and ionize the semiconductor material causing the electrons have high energy to break free of their atomic bonds. Then, the electrons are forcely move in one direction which create a flow of electric current [7]. The layers are placed within the cell opposite charges to prevent the negatively charged electron return to positively the positively charged holes. However, the electrons can move back to the positively charged holes by flowing through the external circuit, thus causing the electricity to flow [8].

The 'p' and 'n' types of semiconductor which are similar to 'positive' and 'negative' because of their plenty of holes or electrons are sandwiched together [9]. When the p-type and n-type semiconductors are joined together, the extra electrons in the n-type material move to the p-type, and the holes thereby empty during this process move to the n-type. These two semiconductors act as a battery since there is flow of hole and electron, thus creates an electric field at the surface where they clash (junction). Figure 2.1 illustrates the detail of electron and hole at n-layer and p-layer.
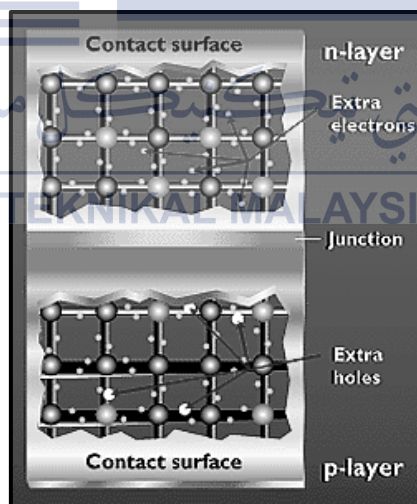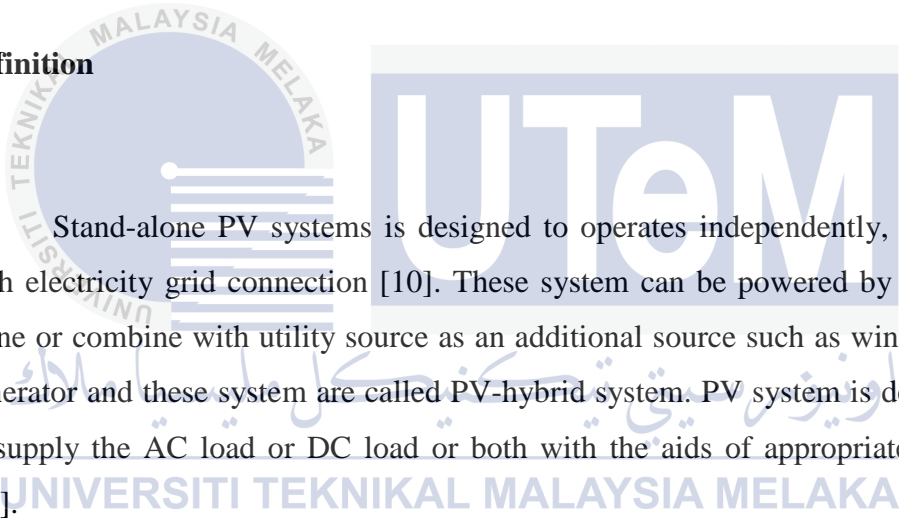

Figure 2.3: Basic Structure of Semiconductors [9]

The rate of electric carriers generation depends on the flux of incident light and the capacity of absorption of the semiconductor. The capacity of absorption depends

mainly on the semiconductor band gap, on the reflectance of the cell surface (that depends on the shape and treatment of the surface), on the intrinsic concentration of carriers of the semiconductor, on the electronic mobility, on the recombination rate, on the temperature, and on several other several factors [4].

2.3   Stand-alone PV System

2.3.1   Definition

Stand-alone PV systems is designed to operates independently, not involving with electricity grid connection [10]. These system can be powered by PV generator alone or combine with utility source as an additional source such as wind and engine-generator and these system are called PV-hybrid system. PV system is designed either to supply the AC load or DC load or both with the aids of appropriate components [11].

Stand-alone PV system is used worldwide and it is the most popular system compare to other PV system. Stand-alone PV system mostly installed to a totally mains-isolated application as the energy provided is enough to power the application [12]. The installation of stand-alone PV system is not only popular in the town area, besides that it is also popular in the remote rural area [13]. Especially the remote locations where the connection to the electricity grid is either not possible or expensive. They are most cost effective when electricity requirements are relatively low. Stand alone systems include a battery bank, inverter, battery charger and a fuel generator set [5].

2.3.2 Configurations

Designing the stand-alone PV system configurations needs a confirmation of which components to connect in the system. The components used depend on the type of the loads (AC or DC load, heavy or light), load requirement (critical oc noncritical, reliability, cost), and its geographical location [14]. The additional equipments as a balance of the system and safely transmit the electricity to the load.

The main component in the system is PV array. It will convert the solar energy into electricity. As the energy generation and consumption do not generally coincide, energy storage is required in most stand-alone systems [15]. The solar energy generated during daylight is not fixed, it change depends on the intensity of the sunlight. Energy need to be stored to ensure the stability of the system. Charge controller is important as it consist of DC/DC converter that will take optimum power from PV array and adjust it to the charge voltage of the battery. Inverter is needed when the type of load is AC load. Since the output power drive from PV is in DC, thus inverter converts the DC power to AC power to feed the AC load.
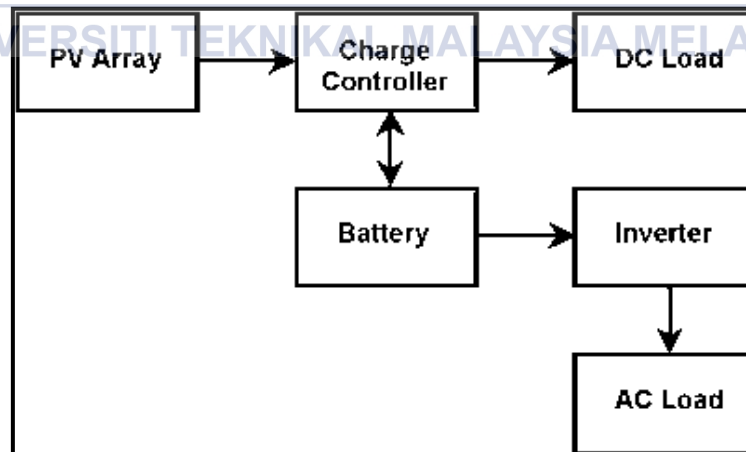

Figure 2.4: Stand-Alone PV System With DC And AC Loads [16]

2.4 Load-shedding Strategy

2.4.1 Definition

Energy efficiency has become an issue debates where several factors may disrupt the effiency of the system such as deregulation of electrical energy distribution, the increasing price of electricity, and the implementation of rolling blackouts [17]. These factors affect the stability of the whole power system. For example when a sudden large industrial load is switched on, it will disrupt the grid system and the system become unstable. Particularly, the differences between the generated power and the load demand caused by disturbance which reduces the generation capacity of the system, thus affect the frequency of the system. The voltages become unstable when the power system unable to meet the reactive power demands of the loads [18].
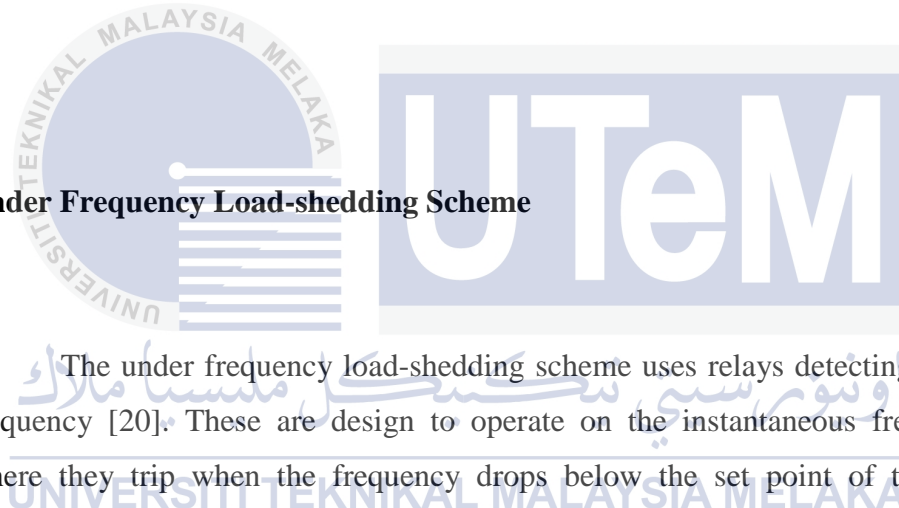
The stability of the system need to be control where the load-shedding strategy can be an emergency control operation. The load-shedding strategy is designed to curtail the system load during emergency situation to control the stability of the system [19]. The loads are curtailed until the available generation could supply the remain loads. Load-shedding strategy balances the real and reactive power supply and the load demand in the system to prevent from the excessive frequency or voltage decline.

The location bus for the load-shedding will be determined based on the load importance, cost, and distance to the contingency location. The acceptable algorithms are developed based on the number of LS steps, amount of load that should be shed in each step, the delay between the stages, and the location of shed load.

2.4.2   Load-shedding Techniques

An automatic load-shedding for power system using different schemes such as under frequency, under voltage and combinations of the two can be employed to avoid frequency or voltage collapse during a significant imbalance between generation and load [19]. These types of load-shedding methods are very dependant on offline studies of the system's dynamic performance and only consider the greatest probable imbalance between generation and load. These methods have to coordinated with the protections of the generating units, shunt capacitors and other automatic actions that occur in the system during frequency and voltage variations.

2.4.2.1 Under Frequency Load-shedding Scheme

The under frequency load-shedding scheme uses relays detecting the system's frequency [20]. These are design to operate on the instantaneous frequency value where they trip when the frequency drops below the set point of the relay. The shedding operation is accomplished in the systems distribution or transmission stations where major load feeders can be controlled by tripping of the circuit breakers (CB) automatically. Different settings can be apply in these load-shedding schemes.

Multiple stages can be use in the scheme [19]. The substation loads are prioritised and grouped according to the importance of the load. The relays can be set to control one or more groups of loads and when there is a frequency drop these can be disconnect sequentially where the group with the highest probability being disconnected the last. Each group disconnected should contribute to the system rate of change of frequency decline. If the load to be disconnected is small compared to the

overall imbalance then the contribution will be insignificant and would cause further problems to the systems frequency decline.

Another setting usual for this type of scheme is the time delay [21]. The time may can be required and used usually to avoid any frequency transient dips that could arise in the system. The time delay also avoids unnecessary load shedding by allowing the load or frequency controls in the system to respond to the frequency deviation. However load shedding performed with long time delays should be set appropriately as it will make the system more vulnerable to system stability if eventually load shedding is required. This method will work adequate in a situation where the system frequency decline is slow.
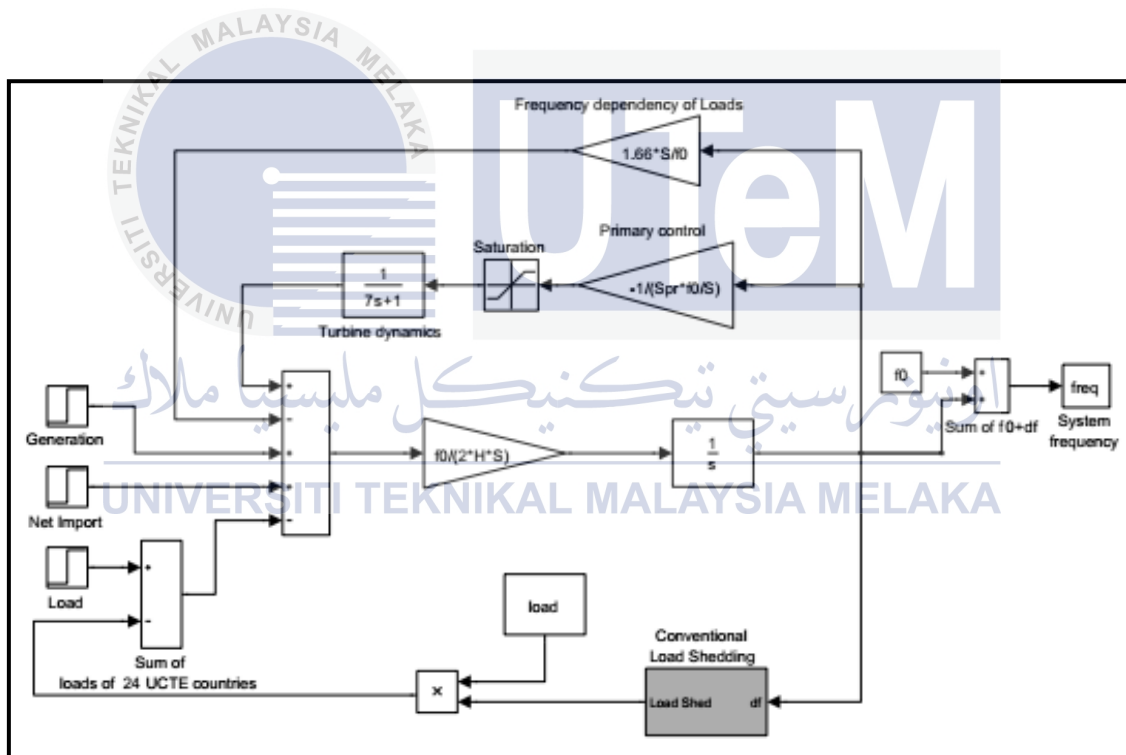
Figure 2.5: Frequency Response Model [19]

2.4.2.2 Under Voltage Load-shedding Scheme

Under voltage load-shedding method has been successfully deployed in transmission systems to protect them from voltage collapse [22]. System studies are required to determine which systems are potential candidates for suitable the under voltage load shedding method. This method is most useful in slow decaying systems where the under voltage load shedding relay time relays can coordinated accordingly and operate to alleviate the system from overload conditions and low voltages.

Voltage collapse can be studied using steady state simulations for the identified areas using a power flow analysis. System planning engineers conduct numerous studies using P-V and Q-V as well as other analytical methods to determine the amount of load required to be shed to preserve voltage stability under different disturbances [23].

Figure 2.6: Example of Q-V Nose Curve [22]
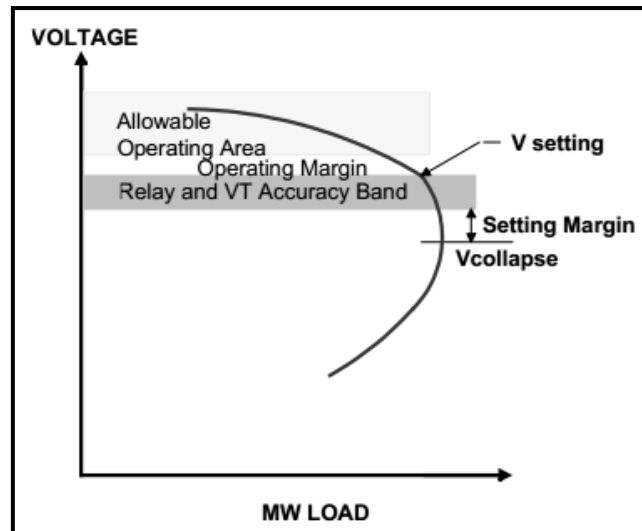
Figure 2.7: Example of P-V Nose Curve [23]
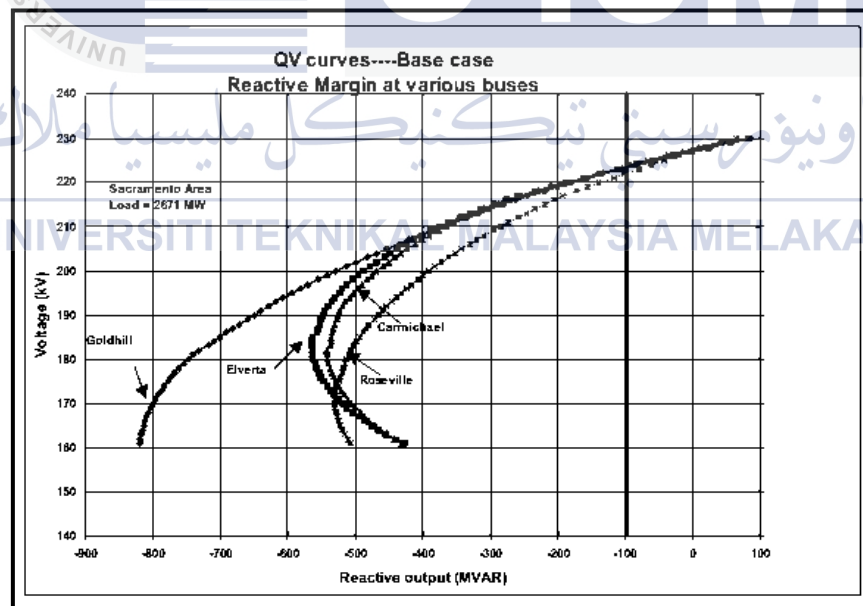
There limitation associated with proper application of under voltage load shedding is the location of its application to where the relaying may be appropriately applied. If it is placed on a distribution line the effects of auto tap changers mask a system overload condition from the relay, or alternatively a line switching operation or the startup of a large industrial plant on one feeder could fool the relay. The relay would not be appropriate at locations directly adjacent to generation powerful enough to control bus voltages even during severe overloads. The relay is best applied to locations with fairly stiff voltages under all normal conditions, so a low voltage condition will reliably indicate a severe overload condition, as may be assumed to be the case at large substations associated with bulk power transmission lines and therefore this method cannot be effectively applied in islanded distribution networks where distribution generation unit power and load demand varies.

2.5 Microgrid Islanded System

2.5.1 Definition

Microgrid is an low voltage (LV) network for examples a small urban area, a shopping center, or industrial park, which the loads and several small modular generation systems are connected to it. Microgrid provides both power and heat to local loads, combine heat and power (CHP) to the system [25]. Besides that, the small modular generation systems can be referred to systems such as photovoltaic (PV), fuel cells, microturbines (MT), small wind turbines (WT) and storage devices (Fly wheels, super capacitors, batteries, and so on), which are lead to a new energy system paradigm [26].

There are two different operating conditions of Microgrid system. The first one is the Normal Interconnected Mode where the Microgrid is connected to a main MV network, either being supplied by it or injecting some amount of power into the main system [25, 26]. The second one is the Emergency Mode where the Microgrid operates autonomously, in a similar way to physical islands, when the disconnection from the upstream MV network occurs due to planned or unplanned events for examples, maintenance actions or faults in the MV network, respectively. Figure 2.8 illustrates the Microgrid system.

Microgrid can operates either in grid connected or islanded operation mode. In the Microgrid management, it requires the balance between supply and demand of power. The Microgrid exchanges power to an interconnected grid to meet the balance during the grid-interconnected mode. On the contrary, during islanded mode, the microgrid should meet the balance using the decrease in generation or load shedding [27].
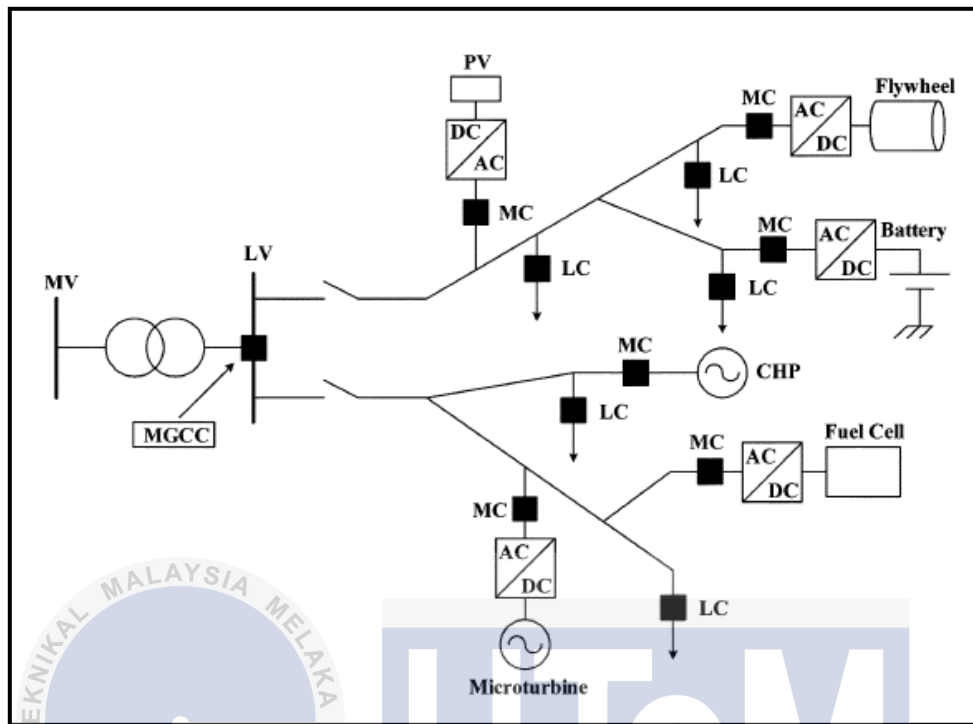
Figure 2.8: Microgrid Architecture, Comprising MS, Loads and Control Device
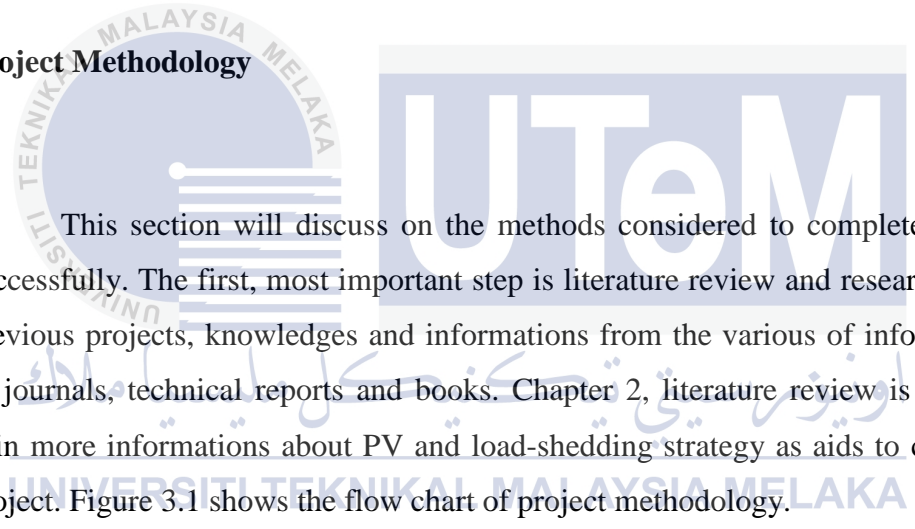
CHAPTER 3

DESIGN METHODOLOGY

3.1   Project Methodology

This section will discuss on the methods considered to complete this project successfully. The first, most important step is literature review and research on related previous projects, knowledges and informations from the various of information such as journals, technical reports and books. Chapter 2, literature review is important to gain more informations about PV and load-shedding strategy as aids to complete this project. Figure 3.1 shows the flow chart of project methodology.

After gaining a lot of informations related to the project, the circuit and PCB layout for hardware is designed by using CadSoft Eagle PCB Design Software. Then the hardware is setup with two inputs, the first one is multiple AC-DC power adaptor as an utility supply, and the second one is solar panel as a PV supply. After finish setup, the connection will be test for the functional of the system.

The algorithms for controlling the loads which depends on the supply is developed in the Arduino IDE. These algorithms will decide which loads will on depends on the acceptable power range of the supply. This coding must be suitable and can work well when implemented with the hardware.
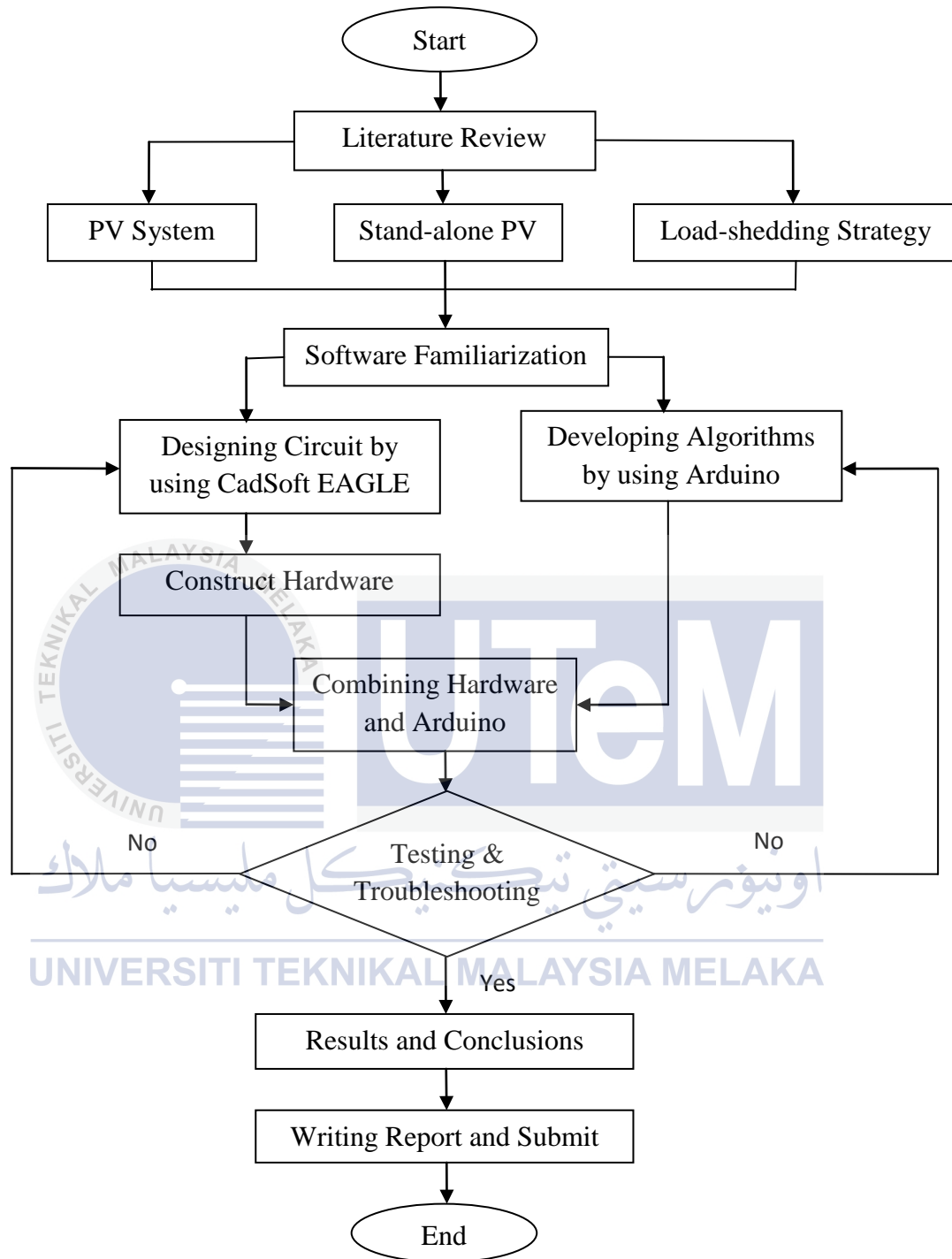
Figure 3.1: Project Methodology

After the implementation of the coding with the hardware, both will be tested and troubleshoot to ensure either the combination of both hardware and coding fulfill

the all the specification of the project and achieve its objectives or fail. When the test is success all the relevant results needed are recorded and discussed. The conclusion of whole project is briefly explained.

3.2   Circuit Components and Design
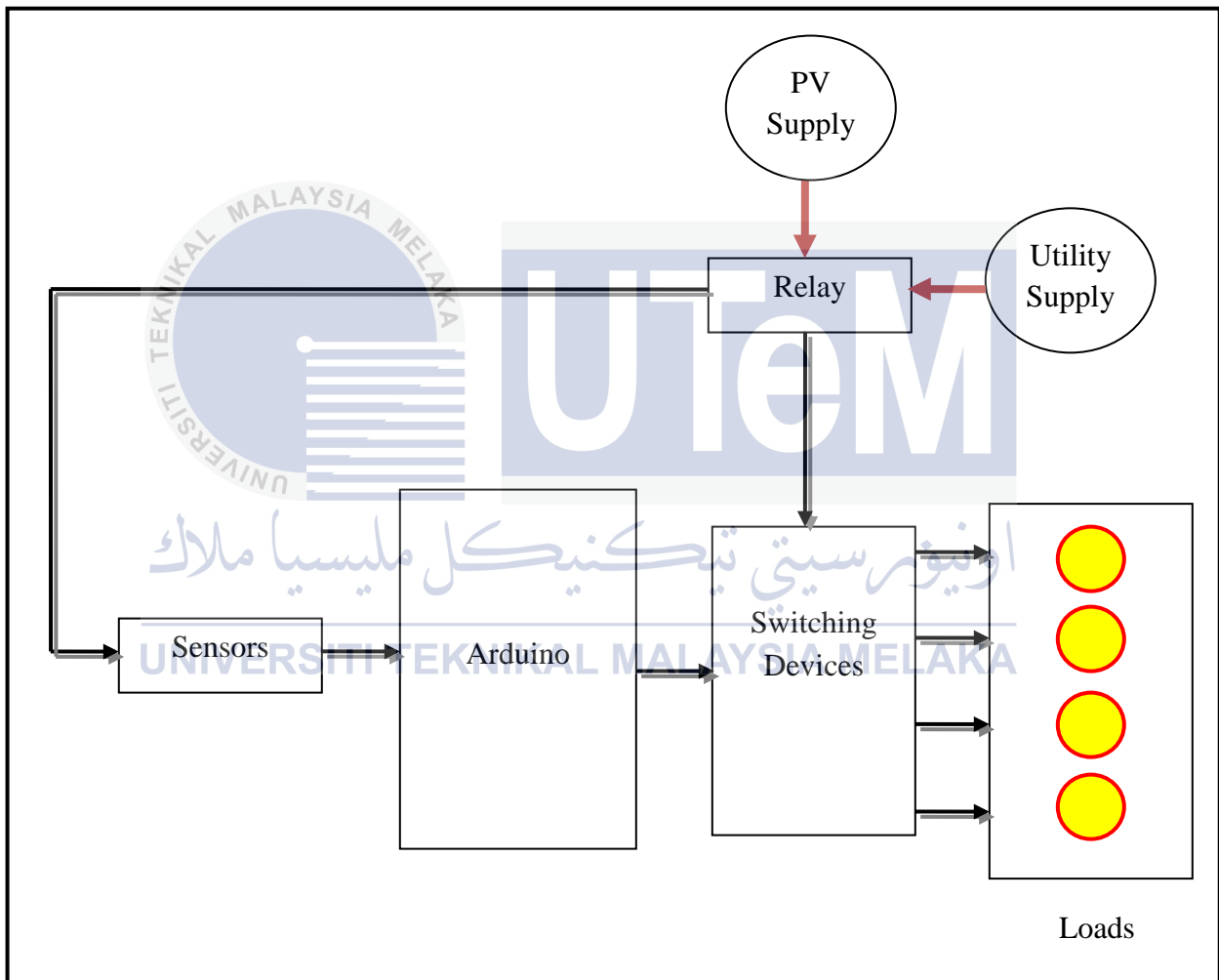
Figure 3.2: Block Diagram of the System

For the whole system, Figure 3.2 briefly illustrates the block diagram of the system. This project is using two supplies, utility supply and PV supply but only one is used at one time. The utility supply is represented by multiple AC-DC power adaptor with rating of 3-12V DC output voltages and 1200mA loading current. The PV supply is from the solar panel with rating of 30W, 18V. Both supplies are connected to a relay where the adaptor is connected to the normally open of relay contactor and PV supply is connected to the normally close of relay contactor. When the adaptor is on, the relay is energized and normally open contact become close therefore, the loads are supplied by the adaptor. Otherwise, PV supply is used to supply the loads if adaptor is off.

A current sensor, ACS712 is connected in series with both supplies to measure the value of currents. Instead of that, voltage divider with resistor value of 15kΩ and 4.7kΩ is used to measure the value of voltage supply. Arduino will received both input values from the sensors and calculate the input power. This input power will be used to determined the number of loads to be shed. The coding programmed in the Arduino are based on the algorithms of input power range and will be compared with power demand by the loads. Arduino will execute the program to control the switching devices by deciding which one will be on and which one will be shed.

The switching devices used are p-channel MOSFETs which are activated by transistors. When Arduino gives high input voltage to transtistor, the transistor will give low signal to the p-channel MOSFET and activate it. Therefore, the load connected to that MOSFET will be on. The main advantages of using p-channel is circuit simplification in medium and low power applications. Arduino will decide which switching device will either on or off.

Four bulbs with rating 6.3V, 3W are used as loads. These bulbs will be light up when the switching devices are activated. By connecting the adaptor which gives 12V voltage supply, all bulbs will be on. However, when PV supply is on, there will be different number of bulbs that are on. The number of bulbs light up or shed depends on the acceptable power range delivered by the PV source.
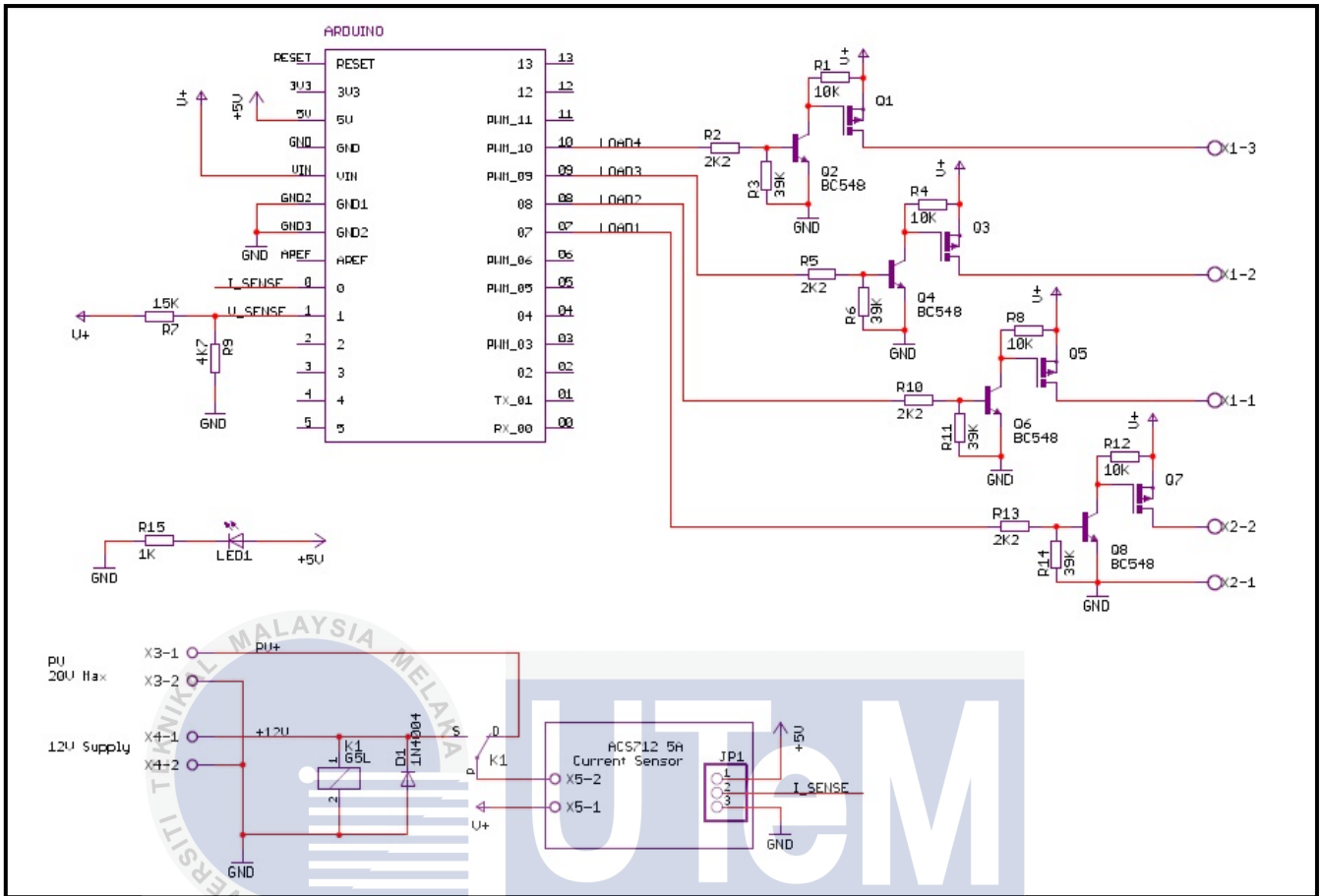
Figure 3.3: Schematic Diagram of the System

Figure 3.3 shows the schematic diagram for the hardware designed in the SoftCad Eagle PCB Design Software. In the figure, the supplies connections are at the bottom left of the corner which connected with the relay. The NA-10 multiple AC-DC power adaptor manufactured by WINSTAR® is used to supply 12V to the loads. Otherwise, if the power adaptor is not functioning, the solar panel will be the power supply. Maximum voltage that can be accepted by this hardware is 20V. The relay used is K1 G5L and the diode 1N4004 is used to protect the system from coil spike when the relay opens. When voltage is applied to a coil it creates a magnetic field. When the voltage is removed the magnetic field collapses and creates a reverse polarity voltage and can be many times the value of the original applied voltage. This creates a transient voltage pulse that can damage other components in the circuit that

are not rated for this polarity or the higher voltage created, things like semiconductors and caps have a maximum voltage limit and breakdown if exceeded. Having a reversed a reversed biased diode across the coil allows the diode to conduct for reverse polarity voltages and creates a short circuit across the coil that allows the pulse to be dissipated in the resistance of the coil wiring.

The ACS712 is a current sensor used to measure the current from the supply. This current sensor is supplied by the 5V from the Arduino board. LED1 is the indicator for the supply, when supply is on the LED1 will on and the color is red. 5V from the Arduino board will supply the LED1. Resistor 1kΩ is for the protection. At the top left of the schematic diagram is the Arduino Uno. Uno will received the voltage and current from the supply and gives signal to the outputs based on the coding inside the Arduino. 15kΩ and 4.7kΩ is the voltage divider to measure the voltage. The maximum voltage it can measure is 20V to ensure it gives less than 5V to Arduino.

The transistor BC548 and the p-channel MOSFET IRF9540 are the switching devices use to on and off the loads. The resistors are used for biasing. The last connection is the load where four bulbs 6.3Vdc, 3W are used. Figure 3.4 shows the PCB layout of the circuit design.
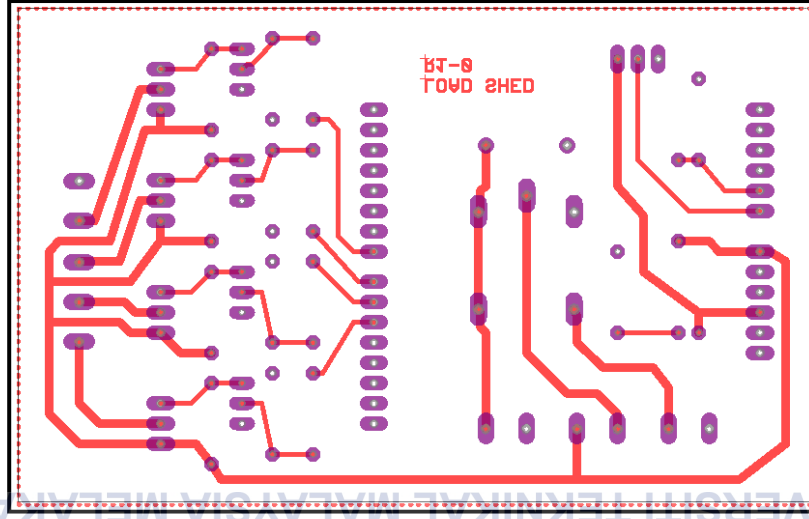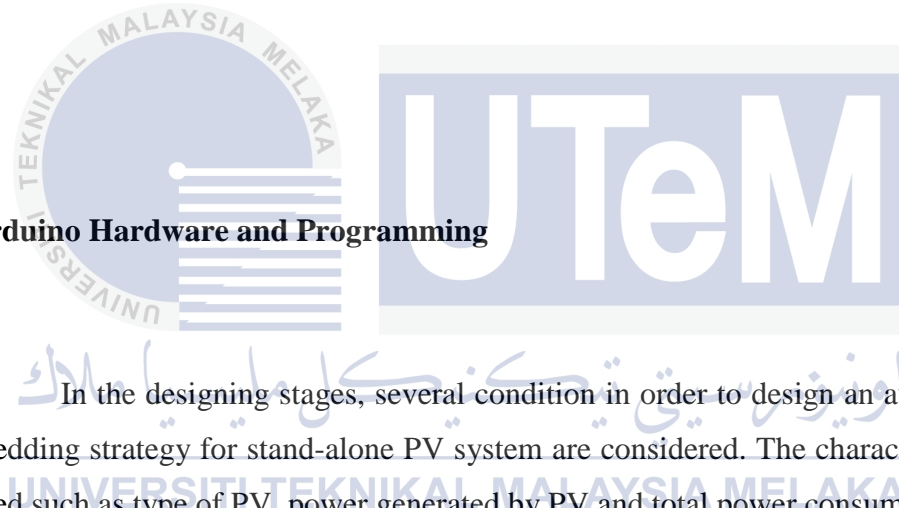

Figure 3.4: PCB Layout of the System

The boards are made from glass reinforced plastic with copper tracks in the place of wires. Components are fixed in position by drilling holes through the board, locating the components and then soldering them in place. The copper tracks link the components together forming a circuit.

The schematic diagram was first converted into a layout of components pin pads, then traces were routed to provide the required interconnections. Pre-printed non-reproducing mylar grids paper assisted in layout, and rub-on dry transfers of common arrangements of circuit elements helped standardize the layout. Traces between devices were made with self-adhesive tape. The finished layout "artwork" was then photographically reproduced on the resist layers of the blank coated copper-clad boards.

3.3   Arduino Hardware and Programming

In the designing stages, several condition in order to design an automatic load-shedding strategy for stand-alone PV system are considered. The characteristics of PV used such as type of PV, power generated by PV and total power consumed by the load are important to set the algorithms for the system. The method for the load-shedding are determined based on the acceptable power range from PV and load demand. Figure 3.5 illustrates the flow of load-shedding operation. The power from the PV is sense and delivered to the Arduino to compare the power of PV, P_{PV} and power of load demand, P_L by using developed algorithms.

The Arduino Uno, shown in Figure 3.5 is chosen as the microcontroller board in this project due to its easy to use benefit. The Arduino is open-source, which means hardware is reasonably priced and development software is free. With the Arduino board, programs can be written and interface circuits can be created to read switches and other sensors, and to control motors and lights with very little effort. Arduino can

sense the environment by receiving input from a variety of sensors and can affect its surroundings by controlling lights, motors, and other actuators.

The Arduino Uno can accept input voltage from 6V to 20V, however, the recommended input voltage range is from 7V to 12V. Users must be reminded that if the external supply source supplied to the Arduino Uno is higher than 12V the board may be suffer from overheating problems. There are pins on the board that can provide output voltage of 5V and 3.3V. The processor provides 32 kilobytes of flash memory, 2 kilobytes of internal SRAM and 1 kilobyte of EEPROM. This microcontroller board provides 14 digital pins that can be used as an input or output. They operate at 5 volts. The Uno has 6 analog inputs, labeled A0 through A5, each of which provide 10 bits of resolution (1024 different values).

The Arduino Uno will be combined with the PCB board of the hardware so that the output data from the Arduino can be sent to the switching devices of the hardware. The analog inputs of Arduino Uno are I_{SENSE} from the current sensor ACS712 at A0 and V_{SENSE} from voltage divider at A1. The supply for Arduino is 9V from the adapter at V_{in} while 5V from the board is supplied to current sensor ACS712 and LED supply indicator. Four digital pins are used as ouputs to connect with the switching devices that control each load.
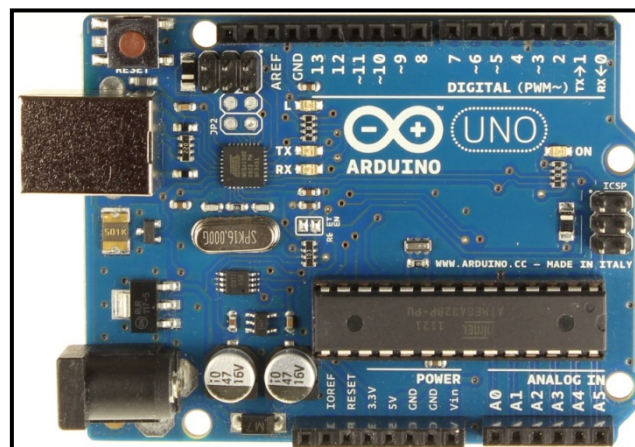

Figure 3.5: Arduino Uno Microcontroller Board

The software used to program the Arduino microcontroller is called Arduino IDE which is available for download from the official Arduino website. Arduino IDE version 1.0.5 is used to write the Arduino codes used in this project. Figure 3.6 shows the flow chart of Arduino programming. When Arduino microcontroller is powered up, it will first read the values from analog inputs where the inputs are current and voltage either from adaptor supply or PV supply. The read values will then be used to calculate the total power draw from the supply by using their respective conversion equation and algorithms.

Rating power for each bulb is 3W which makes the total power for four bulbs are 12W. 12W or more is needed to give maximum power to four bulbs. When there is supply from adaptor, which is 12V, the power supply from adaptor is sufficient enough to support all loads. Thus, all four bulbs will light up when there is supply from adaptor. However, when the adaptor is turned off solar panel will supply all the loads. Because of the power from solar panel is not constant, the load will be shed based on the power range of solar panel.

When the PV supply power more than 12W, all bulbs will be light up. While when the power sensed from PV supply is less than 12W but more than 9W, only three bulb will be light up. Likewise, when the power sensed from PV supply is less than 9W but more than 6W only two bulbs will be light up. When the power sensed from PV supply is less than 6W but more than 3W only one bulb will be light up. When the power sensed from PV supply is too small, no bulb will be light up. Every time the load-shedding operation is done, there will be 5 second delay before the process start over again. Arduino will calculate the power again and do the shedding. This process is repeated until the power supply is off. The full Arduino codes are shown in Appendix.
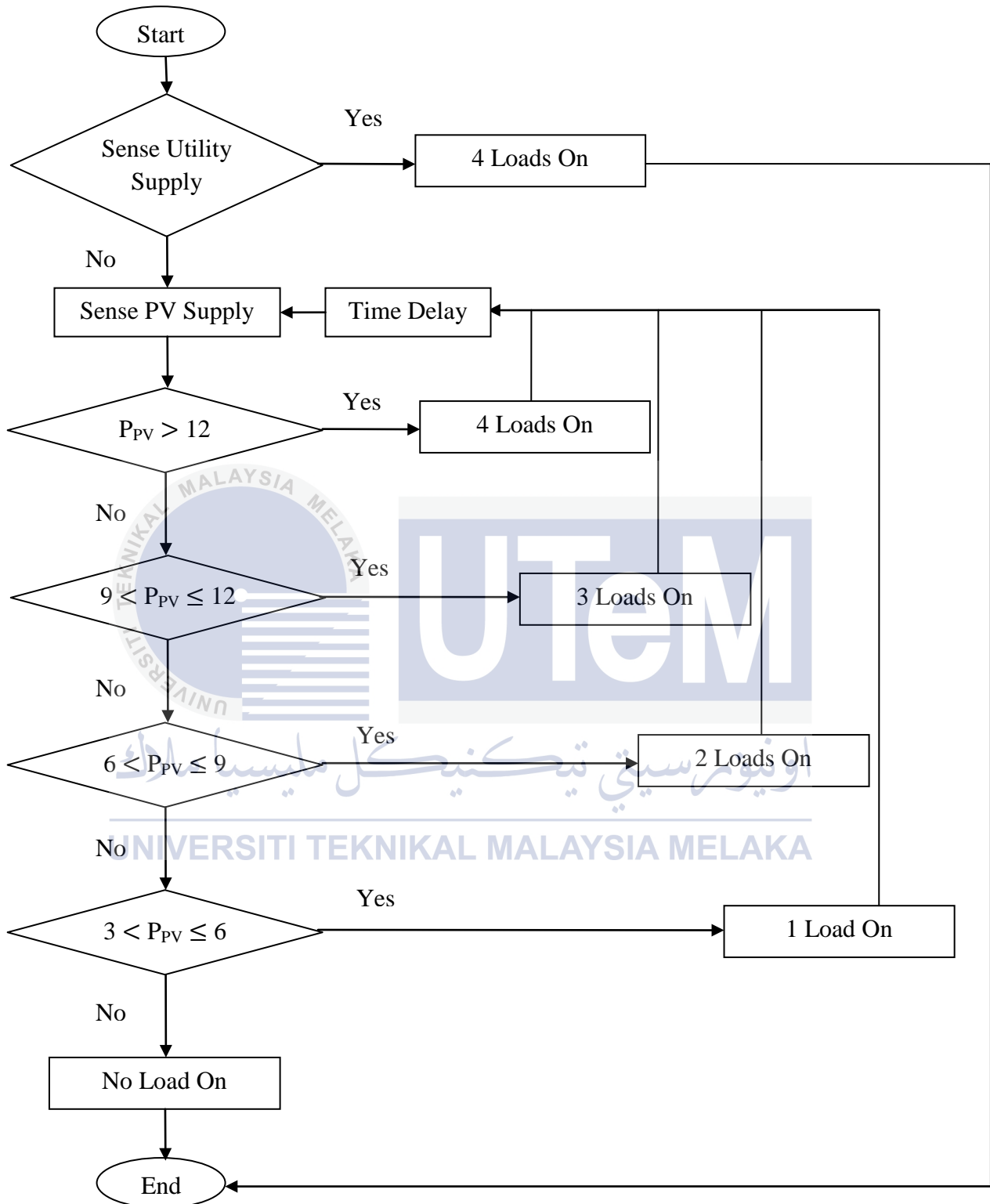
Figure 3.6: Flow Chart of Load-Shedding Operation

CHAPTER 4

RESULTS AND DISCUSSION

4.1 Introduction

This section discusses the results of calibration test results of load-shedding startegy operation using power adaptor and solar panel as power supplies. More importantly, the load-shedding operation is implemented in order to ensure each bulb lighted up in maximum power. Additionally, the full integration of the whole project and screenshots of the project are shown. The load-shedding operation is done in order to give the balance between supply and demand of power.

4.2 Multiple AC-DC Power Adaptor Test Results

Previous projects and research are more focus on larger system applied on a grid. However, this project is just a prototype of the control strategies for microgrids islanded operation in a smaller scope, only to show the operation of load-shedding strategy. Therefore, two supplies are used which the power adaptor is used to represent

the system during the normal condition and the PV supply is used to represent the condition during islanded operation when power failure occur.

Power adaptor will give 12V to the system which has sufficient power to accommodate all four loads. The power supplied by the adaptor is depends on the load and the rating for current is 1.2A. Moreover, all bulbs will light up during power adaptor consumption. Nevertheless, in order to make better understanding about the load-shedding strategy, the multiple AC-DC power adaptor is varies in several values, 4.5V, 6V, 7.5V, 9V, and 12V. In the meantime, the value of power also fluctuate consequently affect the loads. The results of this test is represented in Table 4.1, while Figure 4.1 shows the results of loads and power in form of a graph.

Table 4.1: Table of Multiple AC-DC Power Adaptor Test Results

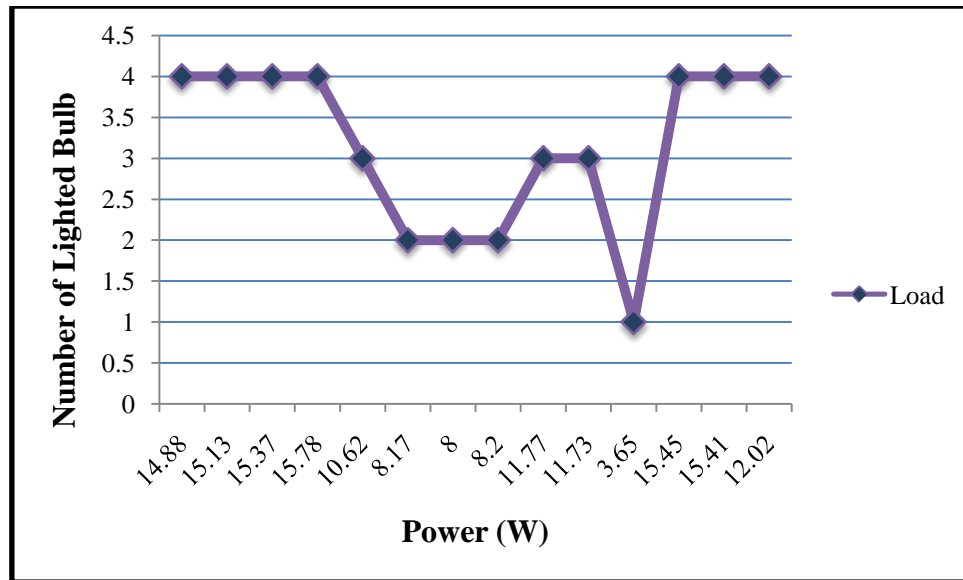| Voltage (V)	Current (A)	Power (W)	Number of Lighted Bulb
7.71	1.93	14.88	4
7.73	1.96	15.13	4
7.85	1.96	15.37	4
7.85	2.01	15.78	4
5.99	1.77	10.62	3
5.24	1.56	8.17	2
5.22	1.53	8	2
5.26	1.56	8.2	2
6.55	1.8	11.77	3
6.52	1.8	11.73	3
4.75	0.77	3.65	1
7.69	2.01	15.45	4
7.67	2.01	15.41	4
6.59	1.82	12.02	4
6.55	1.77	11.6	3

Figure 4.1: Graph of Multiple AC-DC Power Adaptor Test Results

Based from the results in Figure 4.1, there were changes in the number of lighted bulb linearly towards the changes in the value of power sensed from the supply. When the power is greater more loads can be on, while decrease in power will also decrease the numbers of bulbs light up. The highest power sensed by Arduino is 15.78W which is sufficient enough to light up the four loads. While, the lowest power draws from the supply is 3.65W which can light up only one load.

When the voltage of the supply is maintained in 12V, the power will be more than 12W and thus the power is sufficient to maintain light up four bulbs with maximum power. However, when the voltage is decrease to value of 7.5V, the number of bulbs light up also decreased correspond to the decline in value of power to below than 12W. The same thing happened when the voltage is further decrease to smallest value. This operation worked according to the coding programmed in the Arduino.

The advantage of using the multiple AC-DC power adaptor rating 1200mA, DC 3-12V, is the stability of the power produced by the adaptor. This power adaptor has sufficient power to support all four loads. Common adaptors rating below than 800mA are not stable and sufficient enough to support all four loads. Moreover, the adjustable

voltage range make it easier to test the hardware for observing the load-shedding operation.

Each electronic product must have come with its own drawbacks. Although the supply is set to 12V, 9V, 7.5V, 6V and 4.5V, from the Table 4.1 it can be seen that the higher voltage from the supply is 7.85V which is slightly smaller than the value set (12V) because voltage drop happened when connected to the load of the system. As no electronic products are ideal in the real world, different results will be obtained for other set values, where the values might be slightly smaller or larger from the set values. Therefore, the voltages and currents were sensed ten times and only average values are taken for power calculation as programmed in the Arduino.

Besides that, the power adaptor will be overheated if use it in a long period. The power losses of the adaptor will affect the power supply to the bulbs. During overheated period, the power supplied by the adaptor is unstable. The power draw from the overheated adaptor might be smallest from the normal condition. In normal condition, the 12V supply should give sufficient power to all four bulbs. Nevertheless, because of the power losses due to overheated, the power has become smaller and not enough to supply all bulbs. Therefore, the test should be conducted in normal condition in a short period to prevent overheated.

4.3   Solar Panel Test Results

The load-shedding stategy operation is tested again by using solar panel as a power supply. PV systems are low maintenance, provide a cleaner, environmentally friendly alternative, and very reliable source of power. However, the power instability of the PV system can affect the performance of the load. Therefore, load-shedding strategy is an efficient control strategy that can minimize the number of loads depends on the available power supply. To illustrates the influences of irradiant and

temperature on the performance of the solar panel, the tests were executed with different session.

4.3.1 Experiment 1 (Morning Session)

The test was conducted in the morning at 9 a.m. where the wheather is moderate. The power draw from the solar panel is constantly small. The results of this test is represented in Table 4.2, while Figure 4.2 shows the results of loads and power in the form of a graph.

Table 4.2: Table of PV Supply Experiment 1 Results

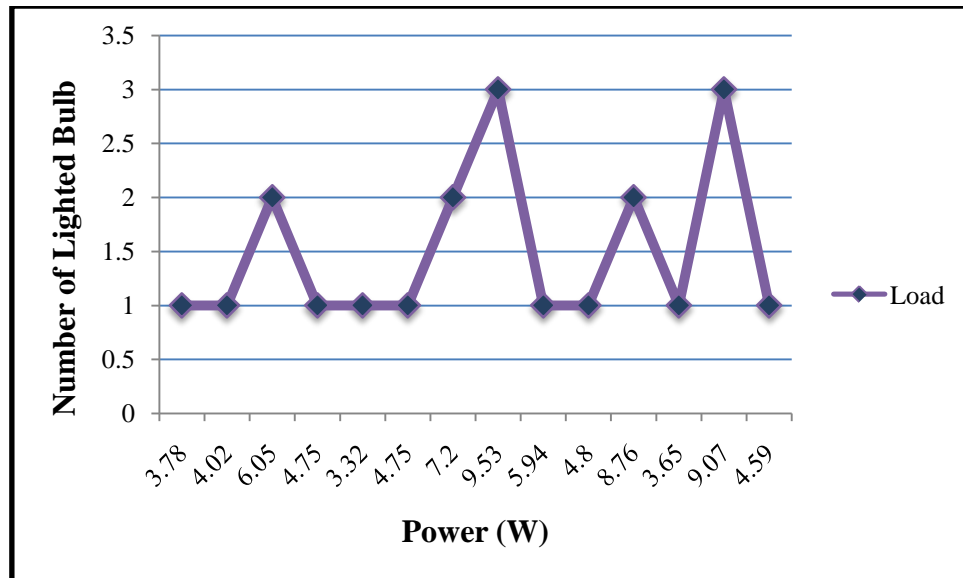| Voltage (V)	Current (A)	Power (W)	Number of Lighted Bulb
4.32	0.88	3.78	1
4.34	0.93	4.02	1
4.66	1.3	6.05	2
4.48	1.06	4.75	1
4.32	0.77	3.32	1
4.48	1.06	4.75	1
4.95	1.46	7.2	2
5.54	1.72	9.53	3
4.58	1.3	5.94	1
4.42	1.09	4.80	1
5.17	1.69	8.76	2
4.75	0.77	3.65	1
5.36	1.69	9.07	3
4.44	1.03	4.59	1
4.32	0.77	3.32	1

Figure 4.2: Graph of PV Supply Experiment 1 Results

Figure 4.2 shows the changes in the number of lighted bulb linearly with the changes in the value of power sensed from the PV supply. From the graph, the powers mostly are small results in the most number of lighted bulb is one only. The maximum number of lighted bulb are three loads which were occured twice. The highest power sensed by Arduino is 9.53W which is sufficient to light up only three loads. While, the lowest power draws from the supply is 3.32W which can light up only one load. The performance of the solar panel is low at this moment as the irradiance of the sun is low at the very moment. It is hardly to produce power more than 9W which can light up three loads not to mention four loads. Thus, more loads need to be shed and from the graph mostly two and three loads are shed because of the deficiency of power.

4.3.2   Experiment 2 (Afternoon Session)

The test was conducted in the afternoon at 12.30 p.m. where the wheather is sunny. The power draw from the solar panel is slightly higher than in the morning. The results of this test is represented in Table 4.3, while Figure 4.3 shows the results of loads and power in the form of a graph.

Table 4.3: Table of PV Supply Experiment 2 Results

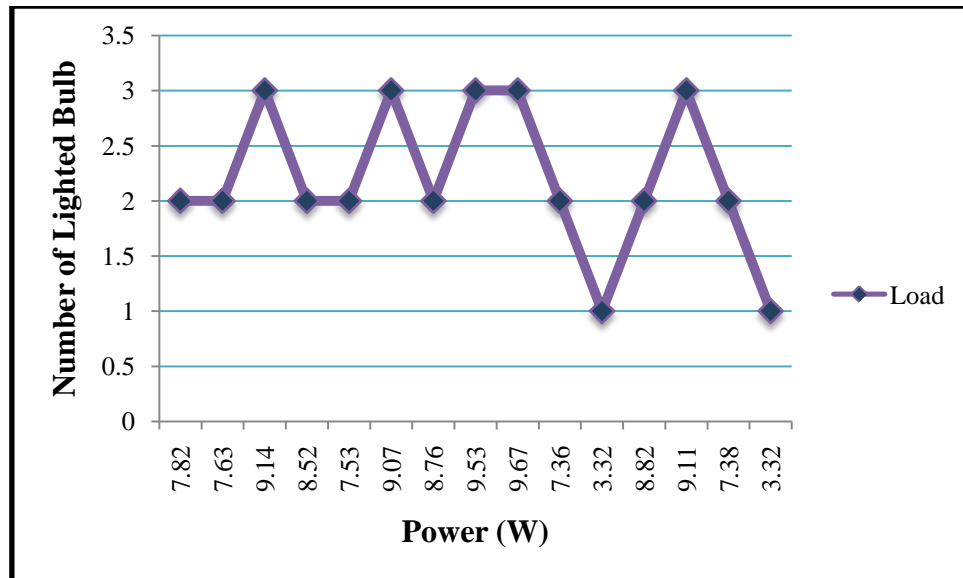| Voltage (V)	Current (A)	Power (W)	Number of Lighted Bulb
4.93	1.59	7.82	2
4.89	1.56	7.63	2
5.32	1.72	9.14	3
5.2	1.64	8.52	2
4.99	1.51	7.53	2
5.28	1.72	9.07	3
5.26	1.67	8.76	2
5.54	1.72	9.53	3
5.62	1.72	9.67	3
4.97	1.48	7.36	2
4.32	0.77	3.32	1
5.38	1.64	8.82	2
5.3	1.72	9.11	3
5.07	1.46	7.38	2
4.32	0.77	3.32	1

Figure 4.3: Graph of PV Supply Experiment 2 Results

The above graph shows the number of lighted bulb and the power generated by PV supply during the sunny afternoon. The correlation between power generated by the PV supply and the number of lighted bulb can be analyzed from the graph. When the power is rised, the number of lighted bulb also increase. During afternoon, the power of PV can reach up to more than 9W because of the high irradiance since it was sunny. Therefore, from the graph it can be seen that the most number of lighted bulb is two and three. This supports the theory that higher irradiances give higher efficiency to the PV supply. When the power is greater more loads can be on, while decrease in power will also decrease the numbers of bulbs light up. The highest power sensed by Arduino is 9.67W which is sufficient to light up the three loads. While, the lowest power draws from the supply is 3.32W which can light up only one load. However, the circumstances where the number of lighted bulb is one, occured twice only. Most of the bulbs light up are about two and three often.

4.3.3 Experiment 3 (Evening Session)

The test was conducted in the evening at 5.30 p.m. where the wheather is partly cloudy. The power draw from the solar panel is slightly lower than in the afternoon. The results of this test is represented in Table 4.4, while Figure 4.4 shows the results of loads and power in the form of a graph.

Table 4.4: Table of PV Supply Experiment 3 Results

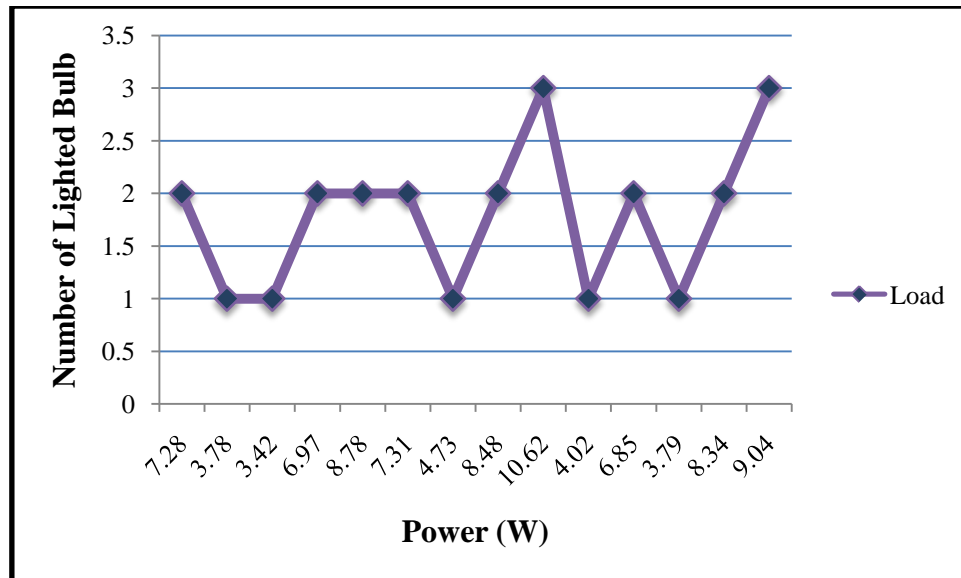| Voltage (V)	Current (A)	Power (W)	Number of Lighted Bulb
4.66	1.56	7.28	2
4.32	0.88	3.78	1
4.30	0.80	3.42	1
4.79	1.46	6.97	2
5.03	1.75	8.78	2
4.85	1.51	7.31	2
4.46	1.06	4.73	1
5.01	1.69	8.48	2
5.99	1.77	10.62	3
4.34	0.93	4.02	1
4.62	1.48	6.85	2
4.34	0.88	3.79	1
4.93	1.69	8.34	2
4.87	1.72	9.04	3
4.87	1.61	7.86	2

Figure 4.4: Graph of PV Supply Experiment 3 Results

From the graph in Figure 4.4, it can be seen that the average power generated by the supply is in the range of 6.85W to 8.78W where the number of lighted bulb is mostly two. The correlation between power generated by the PV supply and the number of lighted bulb can be analyzed from the graph. The highest power sensed by Arduino is 10.62W which is sufficient to light up the three loads. While, the lowest power draws from the supply is 3.42W which can light up only one load. During the test is conducted, the wheather was partly cloudy. The power is not constant and mostly the power generated can only light up one to two loads. Three loads were rarely light up which occur twice only. The performance of the PV in the evening slightly similar to the prformance of the PV during morning. However, the power generated in the evening is slightly higher than that in the morning. Therefore the number of load shed in the evening is less than in the morning. The variation of power might be influenced by the irradiance and the temperature at the moment.

4.4   Combination of Multiple AC-DC Power Adaptor and Solar Panel Test Results

This experiment was conducted using both supplies, power adaptor and PV supply. The experiment is conducted to observe the operation of the system when the power adaptor gave sufficient supply to the loads, however suddenly the power adaptor was off and the PV took over to supply the loads. At this moment, the power from PV might not be sufficient to support the loads, thus the load-shedding strategy operation was executed. Table 4.5 and Figure 4.5 show the result of the system during the usage of power adaptor and PV supply. The operation of load-shedding strategy also can be observed from the table and the graph.

Table 4.5: Table of Combination of Multiple AC-DC Power Adaptor and PV Supply Test Results

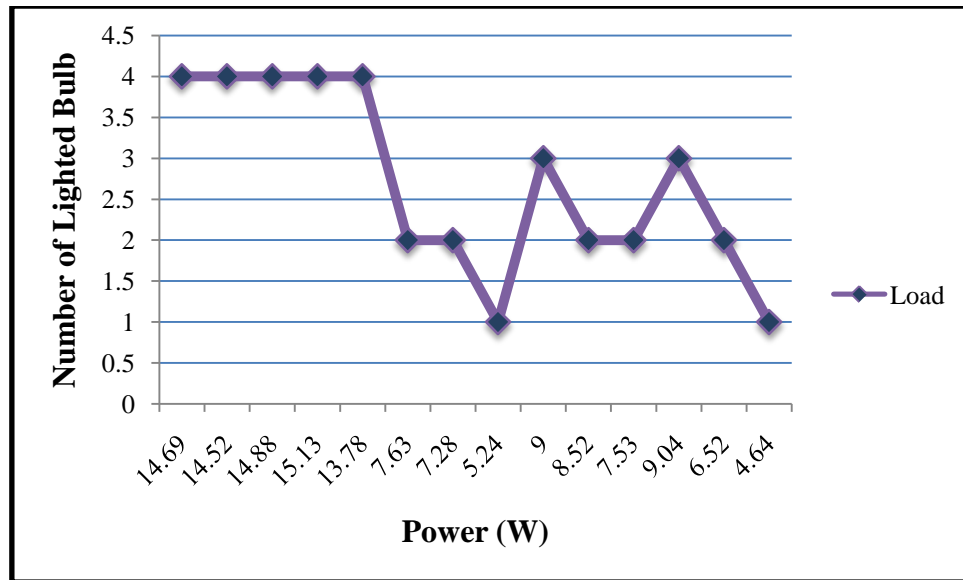| Voltage (V)	Current (A)	Power (W)	Number of Lighted Bulb
7.61	1.93	14.69	4
7.63	1.90	14.52	4
7.71	1.93	14.88	4
7.73	1.96	15.13	4
7.14	1.93	13.78	4
4.89	1.56	7.63	2
4.66	1.56	7.28	2
4.40	1.19	5.24	1
5.32	1.69	9.00	3
5.2	1.64	8.52	2
4.99	1.51	7.53	2
5.26	1.72	9.04	3
4.48	1.46	6.52	2
4.38	1.06	4.64	1
4.62	1.59	7.34	2

Figure 4.5: Graph of Combination of Multiple AC-DC Power Adaptor and PV Supply Test Results

From the graph in Figure 4.5, it can be seen that from the first data up the fifth data, the loads were supplied by the power adaptor. During that time, the number of lighted bulb is four since the power generated from power adaptor is sufficient to support all four loads. The maximum power generated by the adaptor was 15.13W while the minimum power generated was 13.78W which is still can supply the four loads. Suddenly the number of lighted bulb is decreased to two because at this moment, the power adaptor is turned off and at the same time the PV supply is turned on and supply the loads. The graph shows the variation in number of bulb lighted up that occurred because of the values of power generated by the PV supply are not constant. The values of power are depend on the irradiances and the temperature of the surrounding at that moment. From the graph, when the value of power is drop to 4.64W which is the lower power, the three bulb were shed and only one bulb is lighted up. The maximum number of bulbs than can be lighted up is up to three only with the highest power of 9.04W. The load-shedding strategy operation is continue because the power generated keep increasing and decreasing. The performance of the PV supply is less efficient than power adaptor since the maximum loads that PV supply can supports

are up until three loads. Figure 4.6, 4.7, 4.8, and 4.9 show the hardware test results where no load was shed, one load was shed, two loads were shed, and three loads were shed are shown respectively.
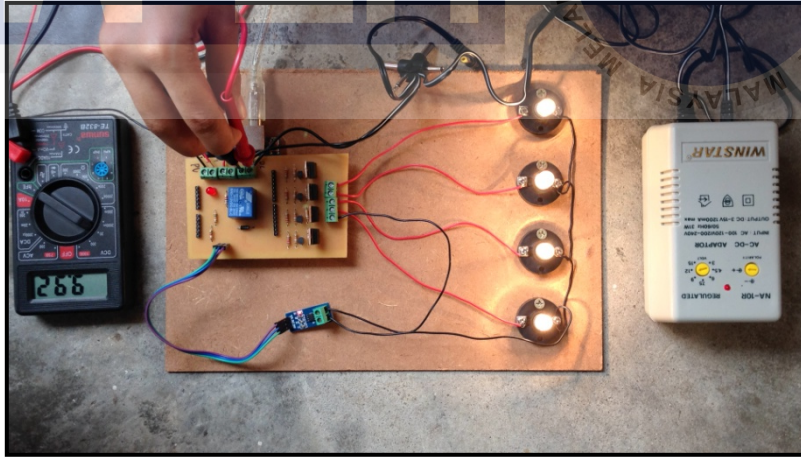

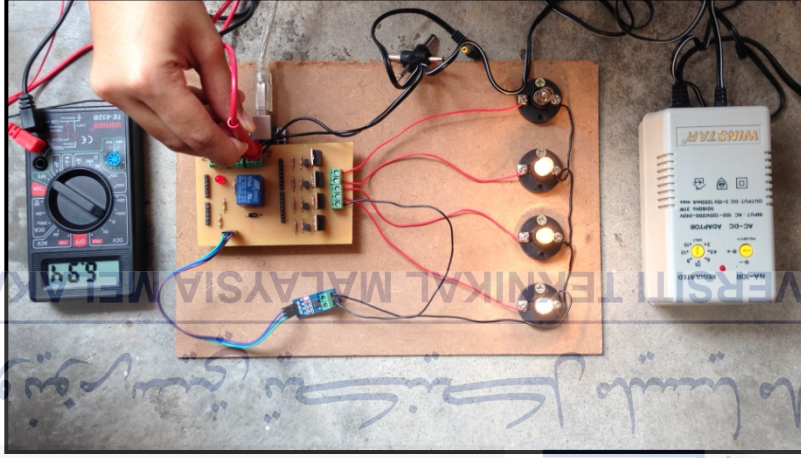Figure 4.6: Result of No Load was Shed Condition
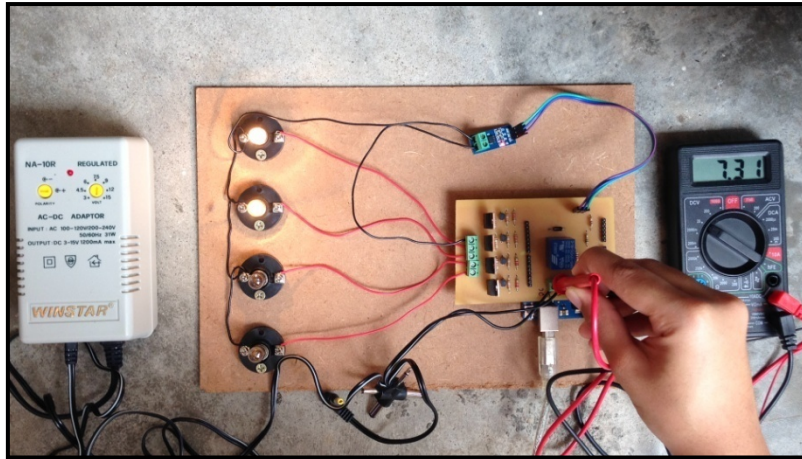

Figure 4.7: Result of One Load was Shed Condition

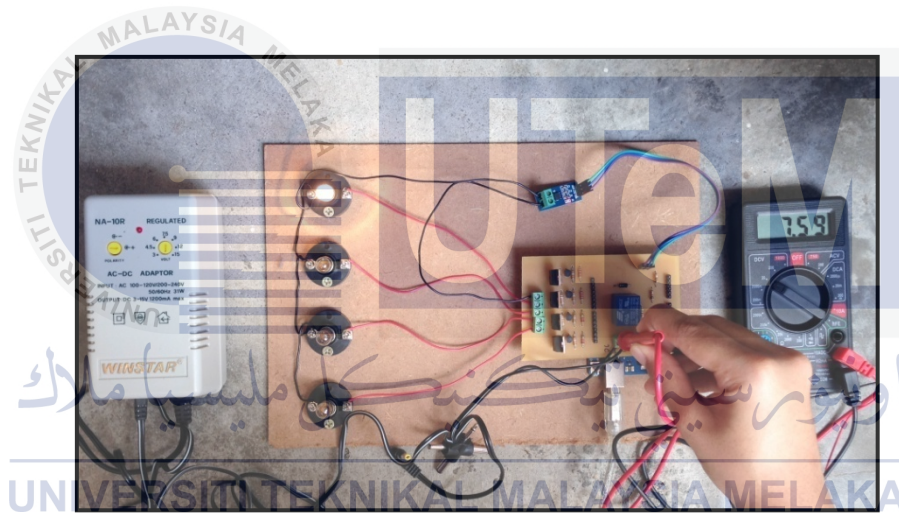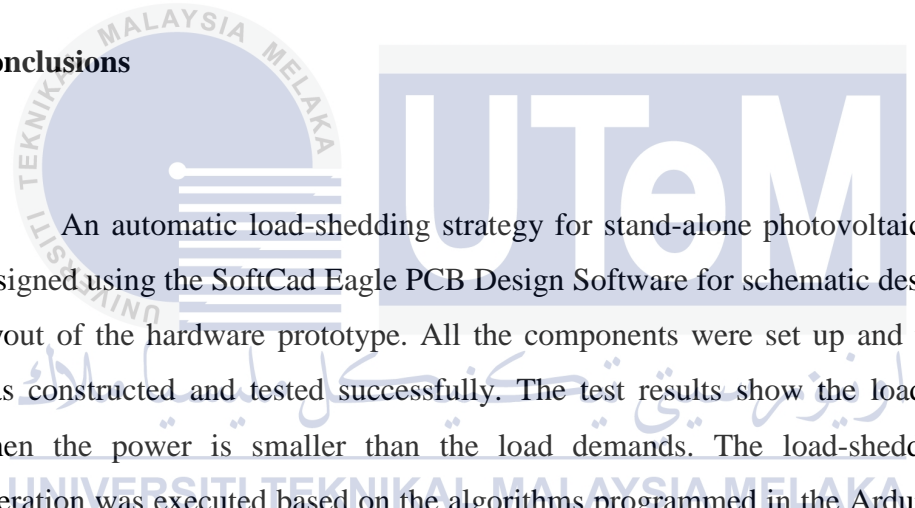**Figure 4.8: Result of Two Loads were Shed Condition**

Figure 4.8: Result of Three Loads were Shed Condition

CHAPTER 5

CONCLUSION AND RECOMMENDATION

5.1   Conclusions

An automatic load-shedding strategy for stand-alone photovoltaic system was designed using the SoftCad Eagle PCB Design Software for schematic design and PCB layout of the hardware prototype. All the components were set up and the hardware was constructed and tested successfully. The test results show the loads been shed when the power is smaller than the load demands. The load-shedding strategy operation was executed based on the algorithms programmed in the Arduino IDE. The algorithms were developed to control the load-shedding operation by using power parameters. The supplies used are multiple AC-DC power adaptor and solar panel which have different performances. The performance of the PV supply is less efficient than power adaptor since the maximum number of bulb that can be lighted up by the PV was three. While the power adaptor can light up all four loads. Solar panel has different power generated within different time, morning, afternoon and evening. Furthermore, the performance of solar was affected by the irradiances of the sun and the surrounding temperatures. The higher value of temperature gives lower efficiency of the PV systems. However, the irradiant is the factor that would make the PV system more efficient where the higher the value of irradiant, the higher the efficiency of the

PV systems. During islanding, the power balance between supply and demand was match at the moment. The results show that the proposed load-shedding scheme can regulate the power supply and the load demand very well. In addition, these results indicate that the load-shedding strategy can contribute to improve the control capability.

5.2   Recommendations

When using one solar panel, all bulbs might not be lighted up with maximum power. This is because the power generated from one solar panel is small. Therefore, to make the system more efficient, two or more solar panel can be used and combined either in parallel or in series to yield better performance.

This system can be installed not just for power failure condition only but might be design for the normal used during daylight to save energy used from the utility. Utility bills also can be saved from the high cost bills by implement this system in the house and improve the performance for daily use during daylight only.

To differentiate between the importance and non-importance load to be shed, the priority of load can be implemented in this system. The load-shedding strategy will be operates on the least important load to the most important load.

REFERENCES

[1]   Inc., N. Z. (July 2003). An Introduction To Photovoltaics.

[2]   S. Sopitpan, P. C. (2000). PV Systems With/Without Grid Back-up for Housing Applications. *IEEE Explore*.

[3]   Compaan, A. (n.d.). *Photovoltaics: Clean Electricity for the 21st Century*. Retrieved October 2013, from APS Physics: http://www.aps.org/publications/apsnews/200504/forefronts.cfm

[4]   Marcelo Gradella Villalva, J. R. (2009). Modelling and Circuit-Based Simulation of Photovoltaic Arrays. *IEEE Xplore*.

[5]   Council, A. C. (n.d.). Photovoltaic (PV) Systems. *Adelaide City Council Green Building Fact Sheets*.

[6]   Solar Energy Industry Association. (n.d.). *Solar Technology*. Retrieved October 2013, from SEIA: http://www.seia.org/policy/solar-technology/photovoltaic-solar-electric

[7]   Association, S. E. (n.d.). *Solar Photovoltaic Technology*. Retrieved October 2013, from SEIA.

[8]   Renewable Energy Systems Ltd. (2000-2013). *How Does It Work?* Retrieved October 2013, from PV Systems: http://www.pvsystems.com/about-solar-pv/how-does-it-work.aspx

[9]   Program, U. D. (n.d.). *How A Photovoltaic Cell Works*. Retrieved October 2013, from About.com Inventors: http://inventors.about.com/library/inventors/blsolar3.htm

[10]   Anca D. Hansen, P. S. (December 2000). Models for a Stand-Alone PV System.

[11] Florida, I. o. (2007). *Types of PV Systems*. Retrieved October 2013, from Florida Solar Energy Center:

http://www.fsec.ucf.edu/en/consumer/solar_electricity/basics/types_of_pv.htm

[12] Luis Castaner, Santiago Silvestre. (March 7, 2003). Standalone PV Systems. In S. S. Luis Castaner, *Modelling Photovoltaic Systems Using Pspice* (pp. 180-182). Chichester West Sussex: John Wiley & Sons Ltd.

[13] Mota, J. A. (2013). A High-Performance Stand-Alone Solar PV Power System for LED Lighting. *ISRN Renewable Energy* .

[14] Solanki, C. S. (July, 2011). Introduction to Solar PV Systems. In *Solar Photovoltaics: Fundamentals, Technologies and Applications* (pp. 391-394). New Delhi: Asoke K. Ghosh, PHI Learning Private Limited.

[15] Society, G. E. (2008). Planning and Designing Stand-alone Systems. In *Planning & Installing Photovoltaic Systems* (pp. 29-39). UK, USA: Earthscan.

[16] Florida, I. o. (2007). *Types of PV Systems*. Retrieved October 2013, from Florida Solar Energy Center:

http://www.fsec.ucf.edu/en/consumer/solar_electricity/basics/types_of_pv.htm

[17] Granderson, A. M. (September 2005). Intelligent Commercial Lighting: Demand-Responsive . *UCEI, University of California Energy Institute* .

[18] Joshi, P. M. (December 2007). LOAD SHEDDING ALGORITHM USING VOLTAGE AND FREQUENCY DATA.

[19] H. Bevrani, A. G. (2010). Power System Load Shedding: Key Issues and New Perspectives. *World Academy of Science, Engineering and Technology 41* .

[20] J.A. Laghari, H. M. (2012). An Intelligent Under Frequency Load Shedding . *IEEE Explore* .

[21] LIMITED, T. N. (2012). Automatic Under-Frequency Load Shedding (AUFLS).

[22] (UVLSTF)*, U. L. (JULY 1999). UNDERVOLTAGE LOAD SHEDDING GUIDELINES. *Western Systems Coordinating Council* .

[23] Mozina, C. (n.d.). UNDERVOLTAGE LOAD SHEDDING. *Beckwith Electric Co., Inc.*

[24] Stephan Koch, S. C. (2010). Mitigation of cascading failures by real-time controlled islanding. *IREP Symposium* .

[25] J. A. Pecas Lopes, Senior Member, IEEE, C. L. Moreira, and A. G. Madureira. (2006). Defining Control Strategies for MicroGrrids Islanded Operation. IEEE **.**

[26] M. Kohansal, M. J. Sanjari, G. B. Gharehpetian. (n.d.). A novel approach to frequency control in an islanded microgrid by load shedding scheduling. IEEE .

[27] Jong-Yul Kim, Member, IEEE, Jin-Hong Jeon, Member, IEEE, Seul-Ki Kim, Member, IEEE, Changhee Cho, Member, IEEE, June Ho Park, Hak-Man Kim, Member, IEEE, and Kee-Young Nam. (2010). Cooperative Control Strategy of Energy Storage System and Microsources for Stabilizing the Microgrid during Islanded Operation. IEEE .

APPENDIX A

Gantt Chart

Activities of project	Final Year Project 1 (2013)					Final Year Project 2 (2014)			
	Sept	Oct	Nov	Dec	Jan	Feb	Mar	Apr	Mei
Literature Review	■	■							
PV analysis by Matlab		■	■						
Circuit design and simulation				■	■				
Analysis and result						■	■		
Report writing								■	■

APPENDIX B

Arduino Coding

```
const byte isn = 0;

const byte vsn = 1;

const byte ld1 = 7;

const byte ld2 = 8;

const byte ld3 = 9;

const byte ld4 = 10;

float current = 0.0;

float voltage = 0.0;

float power = 0.0;

unsigned int current_d = 0;  //digital value for current sensor

unsigned int voltage_d = 0;  //digital value for voltage sensor

void setup ( ) {

pinMode (ld1, OUTPUT); //set output port

pinMode (ld2, OUTPUT);

pinMode (ld3, OUTPUT);

pinMode (ld4, OUTPUT);

digitalWrite (ld1,0);

digitalWrite (ld2,0);

digitalWrite (ld3,0);

digitalWrite (ld4,0);

pinMode (isn, INPUT);
```

```
pinMode (vsn, INPUT);

Serial.begin (9600);

delay (100);

}

void loop() {

 test_load ( );

if (power <= 3)

 {

 digitalWrite (ld1,0);

 digitalWrite (ld2,0);

 digitalWrite (ld3,0);

 digitalWrite (ld4,0);

 Serial.print ("No Load On -- ");

 }

 if (power>3 && power<=6)

 {

 digitalWrite (ld1,1);

 digitalWrite (ld2,0);

 digitalWrite (ld3,0);

 digitalWrite (ld4,0);

 Serial.print ("1 Load On -- ");

 }

 else if (power>6 && power<=9)

 {

 digitalWrite (ld1,1);

 digitalWrite (ld2,1);

 digitalWrite (ld3,0);
```
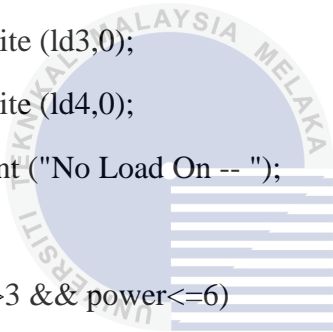
```
  digitalWrite (ld4,0);

  Serial.print ("2 Load On -- ");

 }

 else if (power>9 && power<=12)

 {

 digitalWrite (ld1,1);

 digitalWrite (ld2,1);

 digitalWrite (ld3,1);

 digitalWrite (ld4,0);

 Serial.print ("3 Load On -- ");

 }

 else if (power>12)

 {

 digitalWrite (ld1,1);

 digitalWrite (ld2,1);

 digitalWrite (ld3,1);

 digitalWrite (ld4,1);

 Serial.print ("4 Load On -- ");

 }

 delay(5000);

}

void sensor_read ( ) {

 int voltage_t=0;

 int current_t=0;

 for (int i=0;i<10;++i)  //count total for 10 cycle

 {

  voltage_t = voltage_t + analogRead (vsn);
```

```
 current_t = current_t + analogRead (isn);

 delay (50);

 }

voltage_d = voltage_t/10;  //count average voltage

current_d = current_t/10;  //count average current

voltage = voltage_d * 0.00488; //convert to volt

voltage = voltage * 4.1914;

current = (current_d * 0.00488)-2.527; //sensitivity 185mv/A ACS712

current = current/0.185;

power = voltage * current;

Serial.print ("Volt: ");

Serial.print (voltage);

Serial.print (", Current: ");

Serial.print (current);

Serial.print (", Power: ");

Serial.print (power);

Serial.println (" ");

}

void test_load ( )

{

Serial.print ("Load All On -- ");

digitalWrite (ld1, HIGH);

digitalWrite (ld2, HIGH);   // turn the LED on (HIGH is the voltage level)

digitalWrite (ld3, HIGH);   // turn the LED on (HIGH is the voltage level)

digitalWrite (ld4, HIGH);   // turn the LED on (HIGH is the voltage level)

delay (1000); sensor_read ( );
```

APPENDIX C

1. **Data Sheet of Current Sensor ACS712**

2. **Data Sheet of MOSFET IRF9540**

3. **Data Sheet of Transistor BC548**

Fully Integrated, Hall Effect-Based Linear Current Sensor IC with 2.1 kVRMS Isolation and a Low-Resistance Current Conductor

Features and Benefits

- Low-noise analog signal path
- Device bandwidth is set via the new FILTER pin
- 5 µs output rise time in response to step input current
- 80 kHz bandwidth
- Total output error 1.5% at $T_A = 25°C$
- Small footprint, low-profile SOIC8 package
- 1.2 mΩ internal conductor resistance
- 2.1 kVRMS minimum isolation voltage from pins 1-4 to pins 5-8
- 5.0 V, single supply operation
- 66 to 185 mV/A output sensitivity
- Output voltage proportional to AC or DC currents
- Factory-trimmed for accuracy
- Extremely stable output offset voltage
- Nearly zero magnetic hysteresis
- Ratiometric output from supply voltage

TÜV America
Certificate Number:
U8V 06 05 54214 010

Package: 8 Lead SOIC (suffix LC)
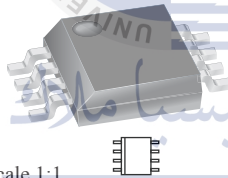
Approximate Scale 1:1

Description

The Allegro™ ACS712 provides economical and precise solutions for AC or DC current sensing in industrial, commercial, and communications systems. The device package allows for easy implementation by the customer. Typical applications include motor control, load detection and management, switch-mode power supplies, and overcurrent fault protection. The device is not intended for automotive applications.

The device consists of a precise, low-offset, linear Hall circuit with a copper conduction path located near the surface of the die. Applied current flowing through this copper conduction path generates a magnetic field which the Hall IC converts into a proportional voltage. Device accuracy is optimized through the close proximity of the magnetic signal to the Hall transducer. A precise, proportional voltage is provided by the low-offset, chopper-stabilized BiCMOS Hall IC, which is programmed for accuracy after packaging.

The output of the device has a positive slope ($>V_{IOUT(Q)}$) when an increasing current flows through the primary copper conduction path (from pins 1 and 2, to pins 3 and 4), which is the path used for current sampling. The internal resistance of this conductive path is 1.2 mΩ typical, providing low power loss. The thickness of the copper conductor allows survival of

Typical Application
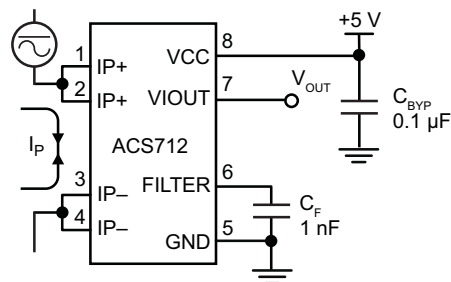
Application 1. The ACS712 outputs an analog signal, V_{OUT}, that varies linearly with the uni- or bi-directional AC or DC primary sampled current, I_P, within the range specified. C_F is recommended for noise management, with values that depend on the application.

ACS712

Fully Integrated, Hall Effect-Based Linear Current Sensor IC with 2.1 kVRMS Isolation and a Low-Resistance Current Conductor

Description (continued)

the device at up to 5× overcurrent conditions. The terminals of the conductive path are electrically isolated from the signal leads (pins 5 through 8). This allows the ACS712 to be used in applications requiring electrical isolation without the use of opto-isolators or other costly isolation techniques.

The ACS712 is provided in a small, surface mount SOIC8 package. The leadframe is plated with 100% matte tin, which is compatible with standard lead (Pb) free printed circuit board assembly processes. Internally, the device is Pb-free, except for flip-chip high-temperature Pb-based solder balls, currently exempt from RoHS. The device is fully calibrated prior to shipment from the factory.

Selection Guide

Part Number	Packing*	T_A (°C)	Optimized Range, I_P (A)	Sensitivity, Sens (Typ) (mV/A)
ACS712ELCTR-05B-T	Tape and reel, 3000 pieces/reel	–40 to 85	±5	185
ACS712ELCTR-20A-T	Tape and reel, 3000 pieces/reel	–40 to 85	±20	100
ACS712ELCTR-30A-T	Tape and reel, 3000 pieces/reel	–40 to 85	±30	66

*Contact Allegro for additional packing options.

Absolute Maximum Ratings

Characteristic	Symbol	Notes	Rating	Units
Supply Voltage	V_{CC}		8	V
Reverse Supply Voltage	V_{RCC}		–0.1	V
Output Voltage	V_{IOUT}		8	V
Reverse Output Voltage	V_{RIOUT}		–0.1	V
Output Current Source	$I_{IOUT(Source)}$		3	mA
Output Current Sink	$I_{IOUT(Sink)}$		10	mA
Overcurrent Transient Tolerance	I_P	1 pulse, 100 ms	100	A
Nominal Operating Ambient Temperature	T_A	Range E	–40 to 85	°C
Maximum Junction Temperature	T_J(max)		165	°C
Storage Temperature	T_{stg}		–65 to 170	°C

Isolation Characteristics

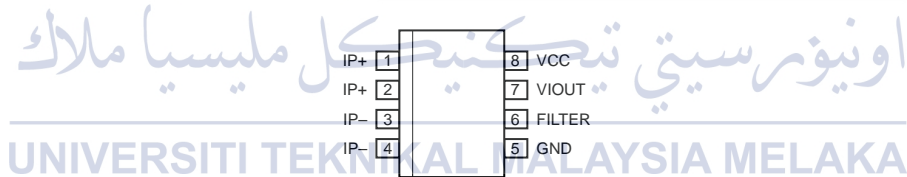| Characteristic	Symbol	Notes	Rating	Unit
Dielectric Strength Test Voltage*	V_{ISO}	Agency type-tested for 60 seconds per UL standard 60950-1, 1st Edition	2100	VAC
Working Voltage for Basic Isolation	V_{WFSI}	For basic (single) isolation per UL standard 60950-1, 1st Edition	354	VDC or V_{pk}
Working Voltage for Reinforced Isolation	V_{WFRI}	For reinforced (double) isolation per UL standard 60950-1, 1st Edition	184	VDC or V_{pk}

* Allegro does not conduct 60-second testing. It is done only during the UL certification process.

Parameter	Specification
Fire and Electric Shock	CAN/CSA-C22.2 No. 60950-1-03 UL 60950-1:2003 EN 60950-1:2001

Allegro MicroSystems, LLC
115 Northeast Cutoff
Worcester, Massachusetts 01615-0036 U.S.A.
1.508.853.5000; www.allegromicro.com

2

ACS712

Fully Integrated, Hall Effect-Based Linear Current Sensor IC with 2.1 kVRMS Isolation and a Low-Resistance Current Conductor

Functional Block Diagram
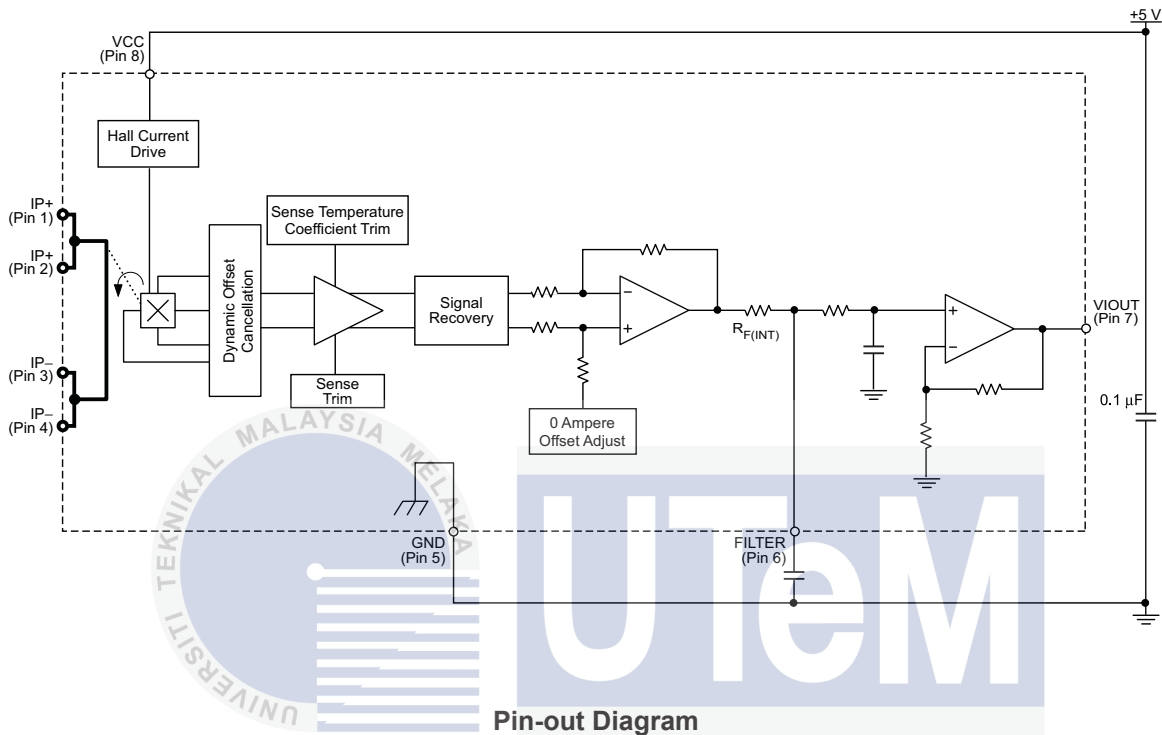
Pin-out Diagram

Terminal List Table

Number	Name	Description
1 and 2	IP+	Terminals for current being sampled; fused internally
3 and 4	IP–	Terminals for current being sampled; fused internally
5	GND	Signal ground terminal
6	FILTER	Terminal for external capacitor that sets bandwidth
7	VIOUT	Analog output signal
8	VCC	Device power supply terminal

Allegro MicroSystems, LLC
115 Northeast Cutoff
Worcester, Massachusetts 01615-0036 U.S.A.
1.508.853.5000; www.allegromicro.com

3

ACS712

*Fully Integrated, Hall Effect-Based Linear Current Sensor IC
with 2.1 kVRMS Isolation and a Low-Resistance Current Conductor*

COMMON OPERATING CHARACTERISTICS[1] over full range of T_A, C_F = 1 nF, and V_{CC} = 5 V, unless otherwise specified

Characteristic	Symbol	Test Conditions	Min.	Typ.	Max.	Units
ELECTRICAL CHARACTERISTICS						
Supply Voltage	V_{CC}		4.5	5.0	5.5	V
Supply Current	I_{CC}	V_{CC} = 5.0 V, output open	–	10	13	mA
Output Capacitance Load	C_{LOAD}	VIOUT to GND	–	–	10	nF
Output Resistive Load	R_{LOAD}	VIOUT to GND	4.7	–	–	kΩ
Primary Conductor Resistance	$R_{PRIMARY}$	T_A = 25°C	–	1.2	–	mΩ
Rise Time	t_r	I_P = I_P(max), T_A = 25°C, C_{OUT} = open	–	3.5	–	µs
Frequency Bandwidth	f	–3 dB, T_A = 25°C; I_P is 10 A peak-to-peak	–	80	–	kHz
Nonlinearity	E_{LIN}	Over full range of I_P	–	1.5	–	%
Symmetry	E_{SYM}	Over full range of I_P	98	100	102	%
Zero Current Output Voltage	$V_{IOUT(Q)}$	Bidirectional; I_P = 0 A, T_A = 25°C	–	V_{CC} × 0.5	–	V
Power-On Time	t_{PO}	Output reaches 90% of steady-state level, T_J = 25°C, 20 A present on leadframe	–	35	–	µs
Magnetic Coupling[2]			–	12	–	G/A
Internal Filter Resistance[3]	$R_{F(INT)}$			1.7		kΩ

[1]Device may be operated at higher primary current levels, I_P, and ambient, T_A, and internal leadframe temperatures, T_A, provided that the Maximum Junction Temperature, T_J(max), is not exceeded.

[2]1G = 0.1 mT.

[3]$R_{F(INT)}$ forms an RC circuit via the FILTER pin.

COMMON THERMAL CHARACTERISTICS[1]

			Min.	Typ.	Max.	Units
Operating Internal Leadframe Temperature	T_A	E range	–40	–	85	°C
					Value	Units
Junction-to-Lead Thermal Resistance[2]	$R_{\theta JL}$	Mounted on the Allegro ASEK 712 evaluation board			5	°C/W
Junction-to-Ambient Thermal Resistance	$R_{\theta JA}$	Mounted on the Allegro 85-0322 evaluation board, includes the power consumed by the board			23	°C/W

[1]Additional thermal information is available on the Allegro website.

[2]The Allegro evaluation board has 1500 mm[2] of 2 oz. copper on each side, connected to pins 1 and 2, and to pins 3 and 4, with thermal vias connecting the layers. Performance values include the power consumed by the PCB. Further details on the board are available from the Frequently Asked Questions document on our website. Further information about board design and thermal performance also can be found in the Applications Information section of this datasheet.

Allegro MicroSystems, LLC
115 Northeast Cutoff
Worcester, Massachusetts 01615-0036 U.S.A.
1.508.853.5000; www.allegromicro.com

4

ACS712

Fully Integrated, Hall Effect-Based Linear Current Sensor IC with 2.1 kVRMS Isolation and a Low-Resistance Current Conductor

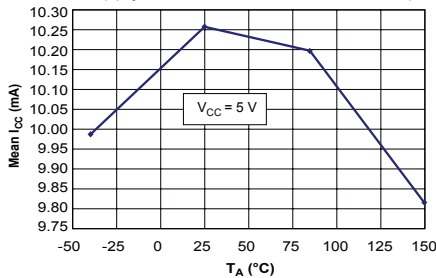| Characteristic	Symbol	Test Conditions	Min.	Typ.	Max.	Units
Optimized Accuracy Range	I_P		–5	–	5	A
Sensitivity	Sens	Over full range of I_P, T_A = 25°C	180	185	190	mV/A
Noise	$V_{NOISE(PP)}$	Peak-to-peak, T_A = 25°C, 185 mV/A programmed Sensitivity, C_F = 47 nF, C_{OUT} = open, 2 kHz bandwidth	–	21	–	mV
Zero Current Output Slope	$\Delta V_{OUT(Q)}$	T_A = –40°C to 25°C	–	–0.26	–	mV/°C
		T_A = 25°C to 150°C	–	–0.08	–	mV/°C
Sensitivity Slope	ΔSens	T_A = –40°C to 25°C	–	0.054	–	mV/A/°C
		T_A = 25°C to 150°C	–	–0.008	–	mV/A/°C
Total Output Error[2]	E_{TOT}	I_P =±5 A, T_A = 25°C	–	±1.5	–	%

[1]Device may be operated at higher primary current levels, I_P, and ambient temperatures, T_A, provided that the Maximum Junction Temperature, $T_{J(max)}$, is not exceeded.

[2]Percentage of I_P, with I_P = 5 A. Output filtered.

Characteristic	Symbol	Test Conditions	Min.	Typ.	Max.	Units
Optimized Accuracy Range	I_P		–20	–	20	A
Sensitivity	Sens	Over full range of I_P, T_A = 25°C	96	100	104	mV/A
Noise	$V_{NOISE(PP)}$	Peak-to-peak, T_A = 25°C, 100 mV/A programmed Sensitivity, C_F = 47 nF, C_{OUT} = open, 2 kHz bandwidth	–	11	–	mV
Zero Current Output Slope	$\Delta V_{OUT(Q)}$	T_A = –40°C to 25°C	–	–0.34	–	mV/°C
		T_A = 25°C to 150°C	–	–0.07	–	mV/°C
Sensitivity Slope	ΔSens	T_A = –40°C to 25°C	–	0.017	–	mV/A/°C
		T_A = 25°C to 150°C	–	–0.004	–	mV/A/°C
Total Output Error[2]	E_{TOT}	I_P =±20 A, T_A = 25°C	–	±1.5	–	%

[1]Device may be operated at higher primary current levels, I_P, and ambient temperatures, T_A, provided that the Maximum Junction Temperature, T_J(max), is not exceeded.

[2]Percentage of I_P, with I_P = 20 A. Output filtered.

Characteristic	Symbol	Test Conditions	Min.	Typ.	Max.	Units
Optimized Accuracy Range	I_P		–30	–	30	A
Sensitivity	Sens	Over full range of I_P, T_A = 25°C	63	66	69	mV/A
Noise	$V_{NOISE(PP)}$	Peak-to-peak, T_A = 25°C, 66 mV/A programmed Sensitivity, C_F = 47 nF, C_{OUT} = open, 2 kHz bandwidth	–	7	–	mV
Zero Current Output Slope	$\Delta V_{OUT(Q)}$	T_A = –40°C to 25°C	–	–0.35	–	mV/°C
		T_A = 25°C to 150°C	–	–0.08	–	mV/°C
Sensitivity Slope	ΔSens	T_A = –40°C to 25°C	–	0.007	–	mV/A/°C
		T_A = 25°C to 150°C	–	–0.002	–	mV/A/°C
Total Output Error[2]	E_{TOT}	I_P = ±30 A, T_A = 25°C	–	±1.5	–	%

[1]Device may be operated at higher primary current levels, I_P, and ambient temperatures, T_A, provided that the Maximum Junction Temperature, T_J(max), is not exceeded.

[2]Percentage of I_P, with I_P = 30 A. Output filtered.

Allegro MicroSystems, LLC
115 Northeast Cutoff
Worcester, Massachusetts 01615-0036 U.S.A.
1.508.853.5000; www.allegromicro.com

5

ACS712

Fully Integrated, Hall Effect-Based Linear Current Sensor IC with 2.1 kVRMS Isolation and a Low-Resistance Current Conductor
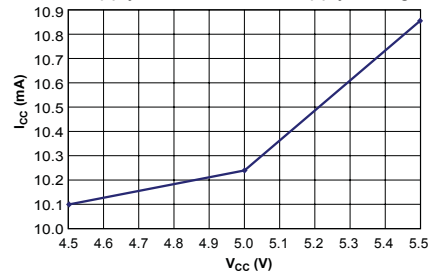
Characteristic Performance
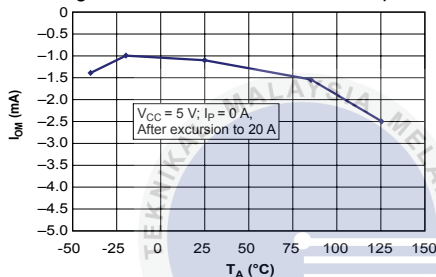
I_P = 5 A, unless otherwise specified

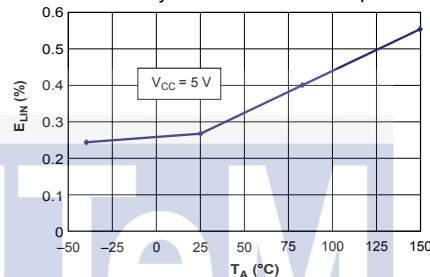Mean Supply Current versus Ambient Temperature

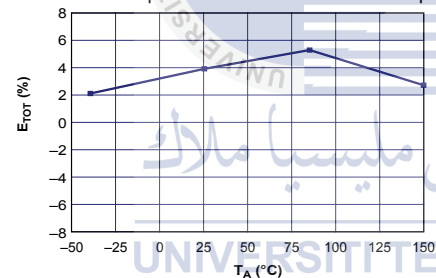
Supply Current versus Supply Voltage
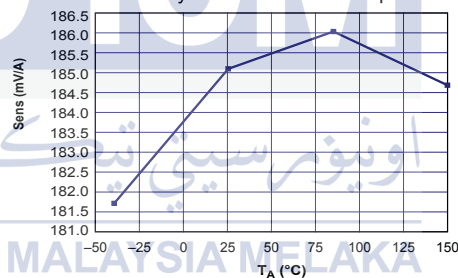

Magnetic Offset versus Ambient Temperature
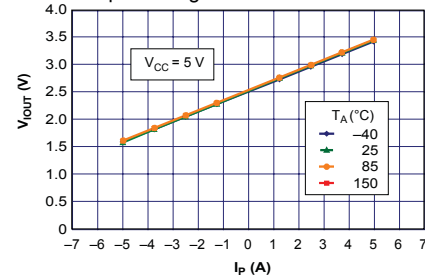

Nonlinearity versus Ambient Temperature
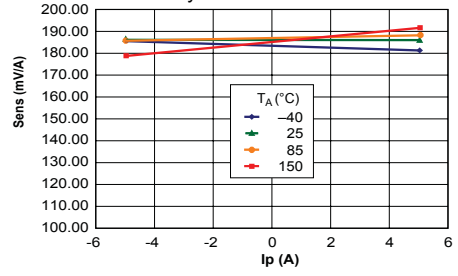

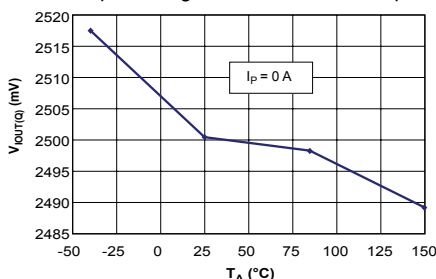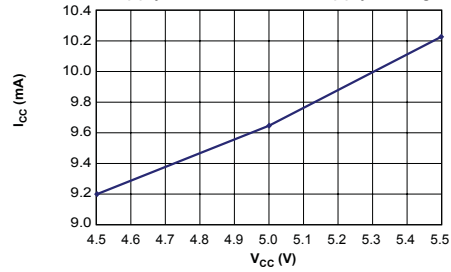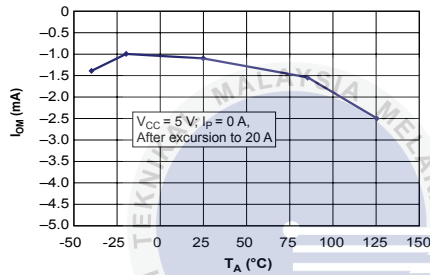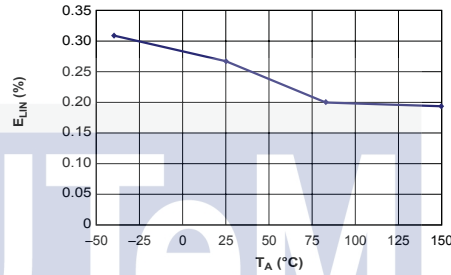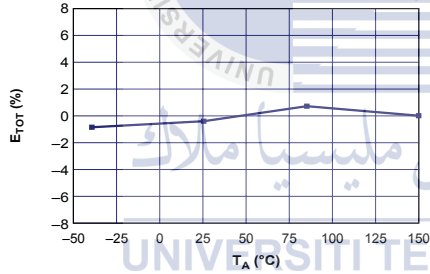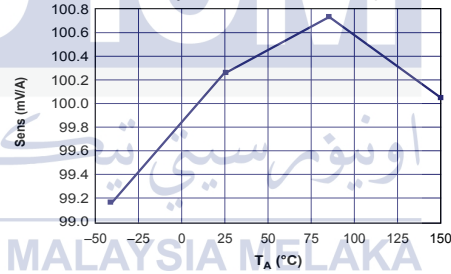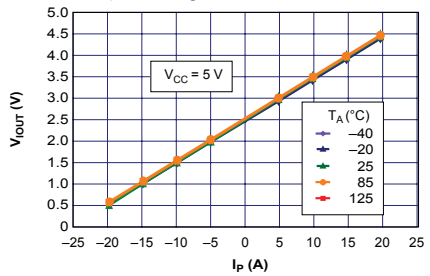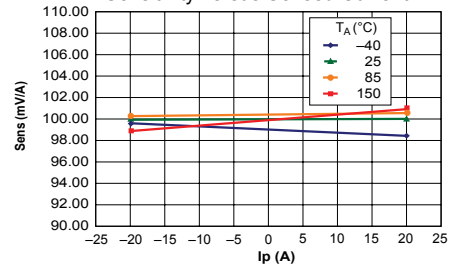Mean Total Output Error versus Ambient Temperature

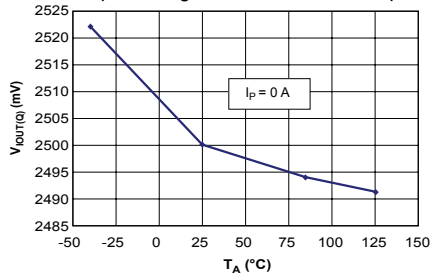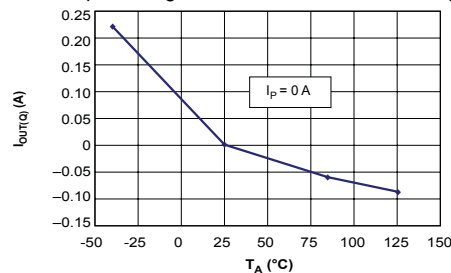Sensitivity versus Ambient Temperature

Output Voltage versus Sensed Current

Sensitivity versus Sensed Current

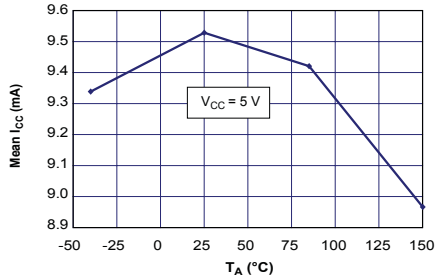0 A Output Voltage versus Ambient Temperature

0 A Output Voltage Current versus Ambient Temperature

ACS712

Fully Integrated, Hall Effect-Based Linear Current Sensor IC with 2.1 kVRMS Isolation and a Low-Resistance Current Conductor
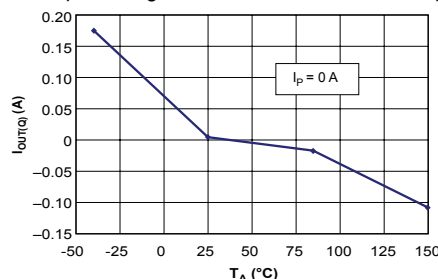
Characteristic Performance

I_P = 20 A, unless otherwise specified
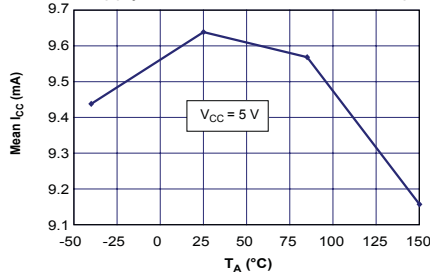
Mean Supply Current versus Ambient Temperature

V_{CC} = 5 V

Supply Current versus Supply Voltage

Magnetic Offset versus Ambient Temperature

V_{CC} = 5 V; I_P = 0 A, After excursion to 20 A

Nonlinearity versus Ambient Temperature

Mean Total Output Error versus Ambient Temperature

Sensitivity versus Ambient Temperature

Output Voltage versus Sensed Current

V_{CC} = 5 V

T_A (°C)
−40
−20
25
85
125

Sensitivity versus Sensed Current

T_A (°C)
−40
25
85
150

0 A Output Voltage versus Ambient Temperature

I_P = 0 A

0 A Output Voltage Current versus Ambient Temperature

I_P = 0 A

ACS712

Fully Integrated, Hall Effect-Based Linear Current Sensor IC with 2.1 kVRMS Isolation and a Low-Resistance Current Conductor

Characteristic Performance

I_P = 30 A, unless otherwise specified

Mean Supply Current versus Ambient Temperature

Supply Current versus Supply Voltage

Magnetic Offset versus Ambient Temperature

Nonlinearity versus Ambient Temperature

Mean Total Output Error versus Ambient Temperature

Sensitivity versus Ambient Temperature

Output Voltage versus Sensed Current

Sensitivity versus Sensed Current

0 A Output Voltage versus Ambient Temperature

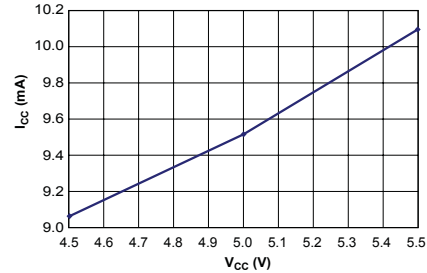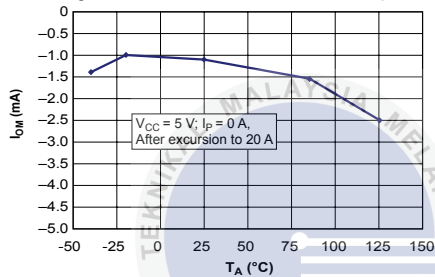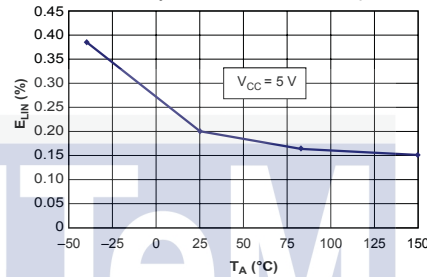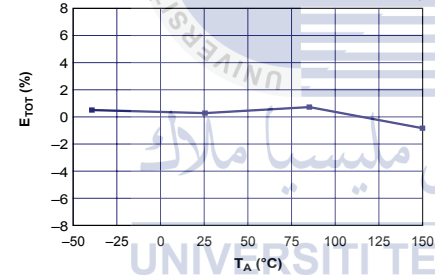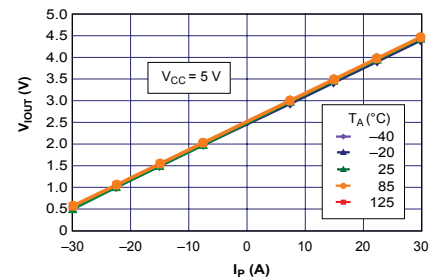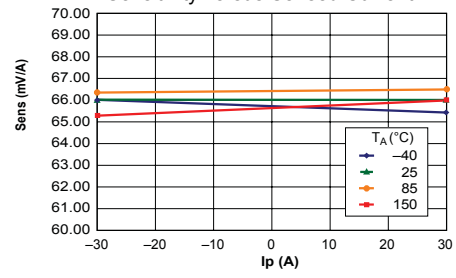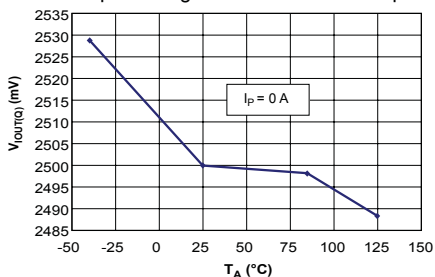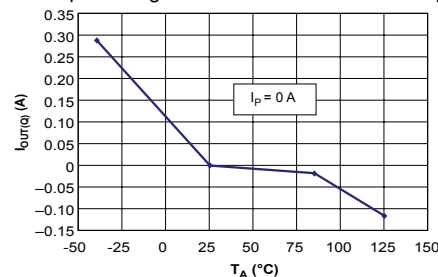0 A Output Voltage Current versus Ambient Temperature

Allegro MicroSystems, LLC
115 Northeast Cutoff
Worcester, Massachusetts 01615-0036 U.S.A.
1.508.853.5000; www.allegromicro.com

8

ACS712

Fully Integrated, Hall Effect-Based Linear Current Sensor IC with 2.1 kVRMS Isolation and a Low-Resistance Current Conductor
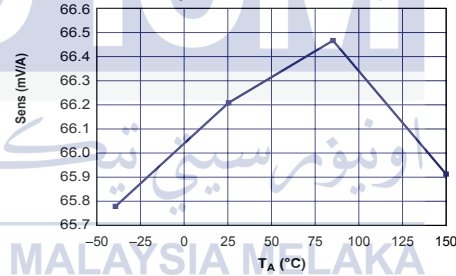
Definitions of Accuracy Characteristics

Sensitivity (Sens). The change in device output in response to a 1A change through the primary conductor. The sensitivity is the product of the magnetic circuit sensitivity (G/A) and the linear IC amplifier gain (mV/G). The linear IC amplifier gain is programmed at the factory to optimize the sensitivity (mV/A) for the full-scale current of the device.

Noise (V_{NOISE}). The product of the linear IC amplifier gain (mV/G) and the noise floor for the Allegro Hall effect linear IC (≈1 G). The noise floor is derived from the thermal and shot noise observed in Hall elements. Dividing the noise (mV) by the sensitivity (mV/A) provides the smallest current that the device is able to resolve.

Linearity (E_{LIN}). The degree to which the voltage output from the IC varies in direct proportion to the primary current through its full-scale amplitude. Nonlinearity in the output can be attributed to the saturation of the flux concentrator approaching the full-scale current. The following equation is used to derive the linearity:

$$100 \left\{ 1 - \left[\frac{\Delta \text{ gain} \times \% \text{ sat } (V_{IOUT\_full\text{-}scale\ amperes} - V_{IOUT(Q)})}{2 (V_{IOUT\_half\text{-}scale\ amperes} - V_{IOUT(Q)})} \right] \right\}$$

where $V_{IOUT\_full\text{-}scale\ amperes}$ = the output voltage (V) when the sampled current approximates full-scale ±I_P.

Symmetry (E_{SYM}). The degree to which the absolute voltage output from the IC varies in proportion to either a positive or negative full-scale primary current. The following formula is used to derive symmetry:

$$100 \left(\frac{V_{IOUT\_+full\text{-}scale\ amperes} - V_{IOUT(Q)}}{V_{IOUT(Q)} - V_{IOUT\_-full\text{-}scale\ amperes}} \right)$$

Quiescent output voltage ($V_{IOUT(Q)}$). The output of the device when the primary current is zero. For a unipolar supply voltage, it nominally remains at $V_{CC}/2$. Thus, V_{CC} = 5 V translates into $V_{IOUT(Q)}$ = 2.5 V. Variation in $V_{IOUT(Q)}$ can be attributed to the resolution of the Allegro linear IC quiescent voltage trim and thermal drift.

Electrical offset voltage (V_{OE}). The deviation of the device output from its ideal quiescent value of $V_{CC}/2$ due to nonmagnetic causes. To convert this voltage to amperes, divide by the device sensitivity, Sens.

Accuracy (E_{TOT}). The accuracy represents the maximum deviation of the actual output from its ideal value. This is also known as the total output error. The accuracy is illustrated graphically in the output voltage versus current chart at right.

Accuracy is divided into four areas:

- **0 A at 25°C.** Accuracy at the zero current flow at 25°C, without the effects of temperature.
- **0 A over Δ temperature.** Accuracy at the zero current flow including temperature effects.
- **Full-scale current at 25°C.** Accuracy at the the full-scale current at 25°C, without the effects of temperature.
- **Full-scale current over Δ temperature.** Accuracy at the full-scale current flow including temperature effects.
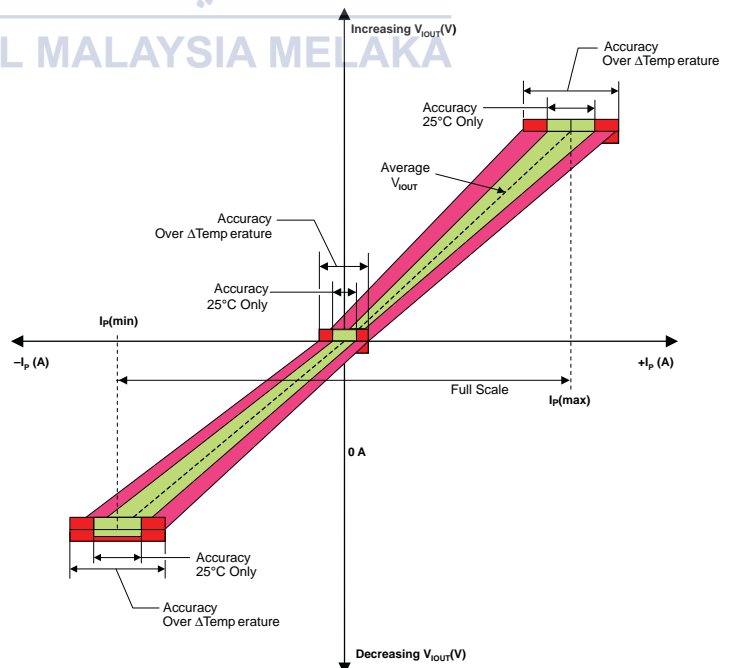
Ratiometry. The ratiometric feature means that its 0 A output, $V_{IOUT(Q)}$, (nominally equal to V_{CC}/2) and sensitivity, Sens, are proportional to its supply voltage, V_{CC}. The following formula is used to derive the ratiometric change in 0 A output voltage, $\Delta V_{IOUT(Q)RAT}$ (%).

$$100 \left(\frac{V_{IOUT(Q)VCC} / V_{IOUT(Q)5V}}{V_{CC} / 5\ V} \right)$$

The ratiometric change in sensitivity, $\Delta Sens_{RAT}$ (%), is defined as:

$$100 \left(\frac{Sens_{VCC} / Sens_{5V}}{V_{CC} / 5\ V} \right)$$

Output Voltage versus Sampled Current
Accuracy at 0 A and at Full-Scale Current

Allegro MicroSystems, LLC
115 Northeast Cutoff
Worcester, Massachusetts 01615-0036 U.S.A.
1.508.853.5000; www.allegromicro.com

9

ACS712

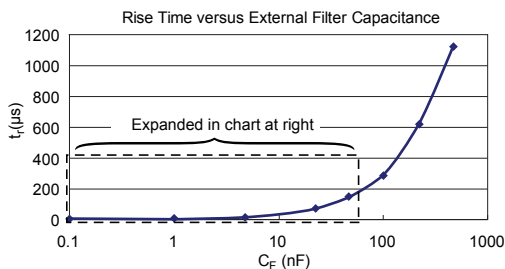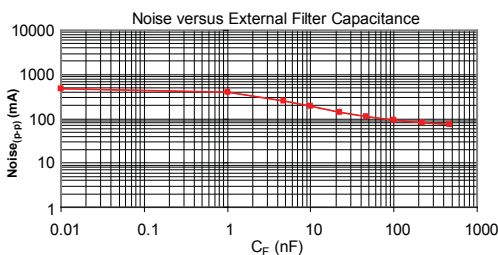*Fully Integrated, Hall Effect-Based Linear Current Sensor IC with 2.1 kVRMS Isolation and a Low-Resistance Current Conductor*
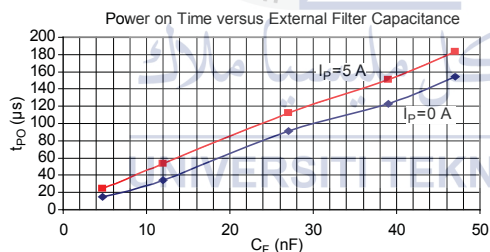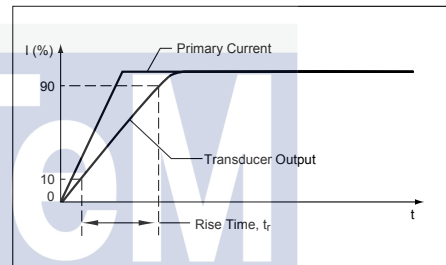
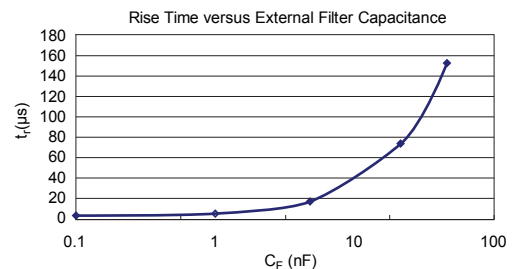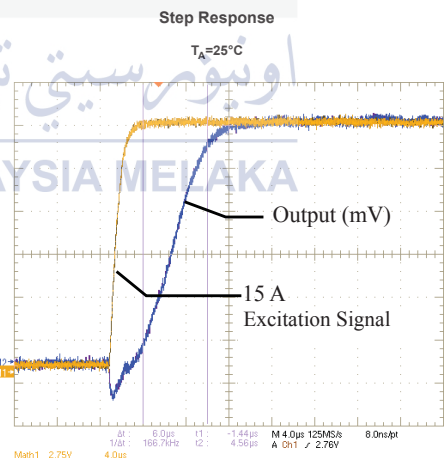## Definitions of Dynamic Response Characteristics

Power-On Time (t$_{PO}$). When the supply is ramped to its operating voltage, the device requires a finite time to power its internal components before responding to an input magnetic field. Power-On Time, t$_{PO}$, is defined as the time it takes for the output voltage to settle within ±10% of its steady state value under an applied magnetic field, after the power supply has reached its minimum specified operating voltage, V$_{CC}$(min), as shown in the chart at right.

t$_1$= time at which power supply reaches minimum specified operating voltage

t$_2$= time at which output voltage settles within ±10% of its steady state value under an applied magnetic field
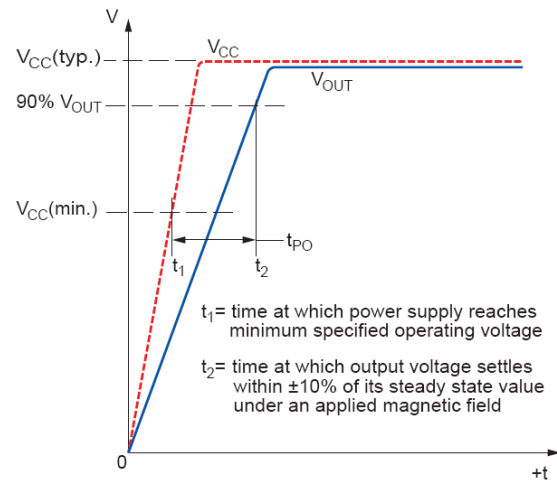
Rise time (t$_r$). The time interval between a) when the device reaches 10% of its full scale value, and b) when it reaches 90% of its full scale value. The rise time to a step response is used to derive the bandwidth of the device, in which $f(–3\ dB) = 0.35/t_r$. Both t$_r$ and t$_{RESPONSE}$ are detrimentally affected by eddy current losses observed in the conductive IC ground plane.

Step Response

T$_A$=25°C

Output (mV)

15 A
Excitation Signal

Power on Time versus External Filter Capacitance

Noise versus External Filter Capacitance

Rise Time versus External Filter Capacitance

C$_F$ (nF)	t$_r$ (µs)
Open	3.5
1	5.8
4.7	17.5
22	73.5
47	88.2
100	291.3
220	623
470	1120

Rise Time versus External Filter Capacitance

ACS712

Fully Integrated, Hall Effect-Based Linear Current Sensor IC with 2.1 kVRMS Isolation and a Low-Resistance Current Conductor
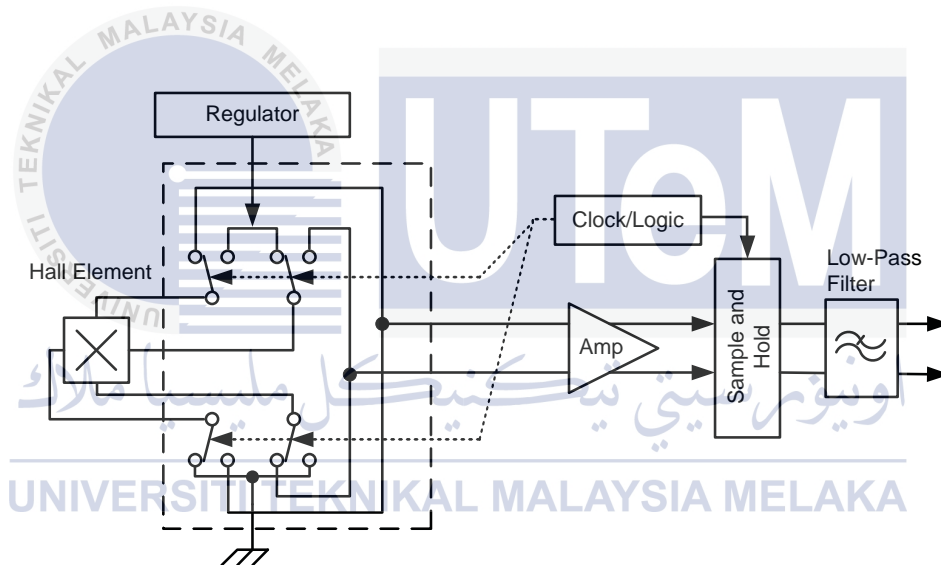
Chopper Stabilization Technique

Chopper Stabilization is an innovative circuit technique that is used to minimize the offset voltage of a Hall element and an associated on-chip amplifier. Allegro patented a Chopper Stabilization technique that nearly eliminates Hall IC output drift induced by temperature or package stress effects. This offset reduction technique is based on a signal modulation-demodulation process. Modulation is used to separate the undesired DC offset signal from the magnetically induced signal in the frequency domain. Then, using a low-pass filter, the modulated DC offset is suppressed while the magnetically induced signal passes through

the filter. As a result of this chopper stabilization approach, the output voltage from the Hall IC is desensitized to the effects of temperature and mechanical stress. This technique produces devices that have an extremely stable Electrical Offset Voltage, are immune to thermal stress, and have precise recoverability after temperature cycling.

This technique is made possible through the use of a BiCMOS process that allows the use of low-offset and low-noise amplifiers in combination with high-density logic integration and sample and hold circuits.

Concept of Chopper Stabilization Technique

Allegro MicroSystems, LLC
115 Northeast Cutoff
Worcester, Massachusetts 01615-0036 U.S.A.
1.508.853.5000; www.allegromicro.com

11

ACS712

Fully Integrated, Hall Effect-Based Linear Current Sensor IC with 2.1 kVRMS Isolation and a Low-Resistance Current Conductor
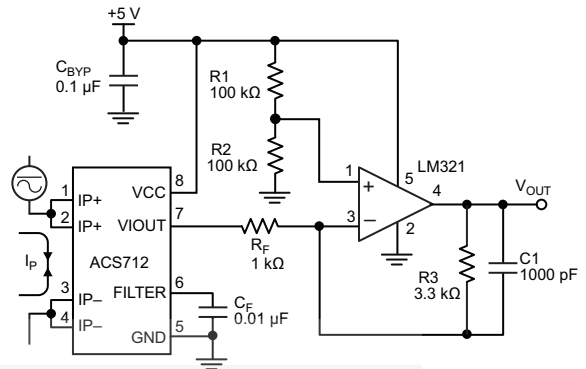
Typical Applications
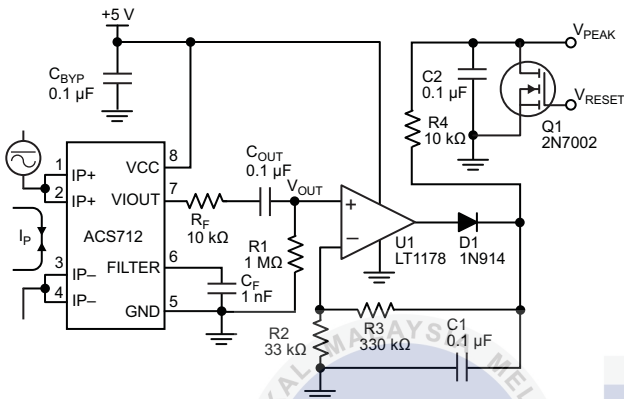
Application 2. Peak Detecting Circuit

Application 3. This configuration increases gain to 610 mV/A (tested using the ACS712ELC-05A).
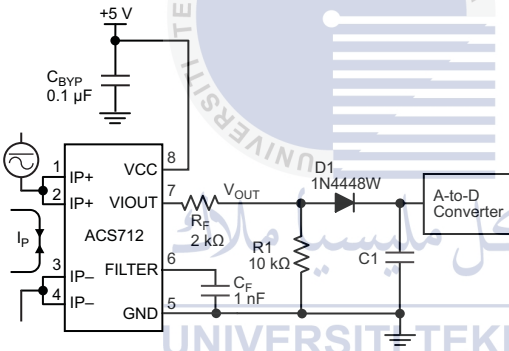
Application 4. Rectified Output. 3.3 V scaling and rectification application for A-to-D converters. Replaces current transformer solutions with simpler ACS circuit. C1 is a function of the load resistance and filtering desired. R1 can be omitted if the full range is desired.
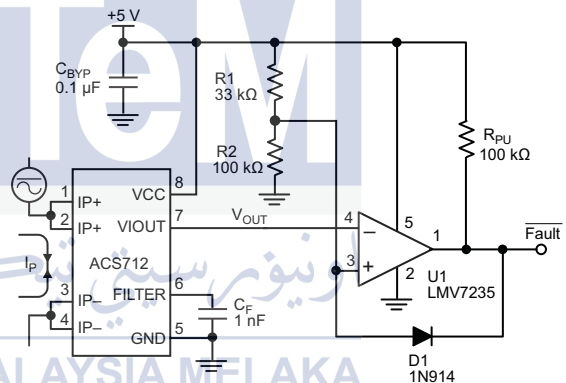
Application 5. 10 A Overcurrent Fault Latch. Fault threshold set by R1 and R2. This circuit latches an overcurrent fault and holds it until the 5 V rail is powered down.

Allegro MicroSystems, LLC
115 Northeast Cutoff
Worcester, Massachusetts 01615-0036 U.S.A.
1.508.853.5000; www.allegromicro.com

12

ACS712

Fully Integrated, Hall Effect-Based Linear Current Sensor IC with 2.1 kVRMS Isolation and a Low-Resistance Current Conductor

Improving Sensing System Accuracy Using the FILTER Pin

In low-frequency sensing applications, it is often advantageous to add a simple RC filter to the output of the device. Such a low-pass filter improves the signal-to-noise ratio, and therefore the resolution, of the device output signal. However, the addition of an RC filter to the output of a sensor IC can result in undesirable device output attenuation — even for DC signals.

Signal attenuation, ΔV_{ATT}, is a result of the resistive divider effect between the resistance of the external filter, R_F (see Application 6), and the input impedance and resistance of the customer interface circuit, R_{INTFC}. The transfer function of this resistive divider is given by:

$$\Delta V_{ATT} = V_{IOUT}\left(\frac{R_{INTFC}}{R_F + R_{INTFC}}\right).$$

Even if R_F and R_{INTFC} are designed to match, the two individual resistance values will most likely drift by different amounts over
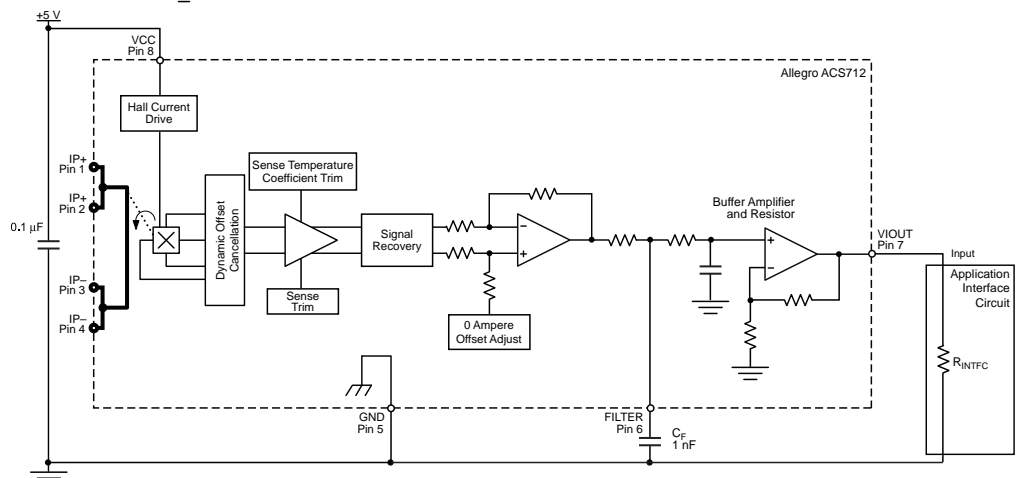
temperature. Therefore, signal attenuation will vary as a function of temperature. Note that, in many cases, the input impedance, R_{INTFC}, of a typical analog-to-digital converter (ADC) can be as low as 10 kΩ.

The ACS712 contains an internal resistor, a FILTER pin connection to the printed circuit board, and an internal buffer amplifier. With this circuit architecture, users can implement a simple RC filter via the addition of a capacitor, C_F (see Application 7) from the FILTER pin to ground. The buffer amplifier inside of the ACS712 (located after the internal resistor and FILTER pin connection) eliminates the attenuation caused by the resistive divider effect described in the equation for ΔV_{ATT}. Therefore, the ACS712 device is ideal for use in high-accuracy applications that cannot afford the signal attenuation associated with the use of an external RC low-pass filter.

Application 6. When a low pass filter is constructed externally to a standard Hall effect device, a resistive divider may exist between the filter resistor, R_F, and the resistance of the customer interface circuit, R_{INTFC}. This resistive divider will cause excessive attenuation, as given by the transfer function for ΔV_{ATT}.
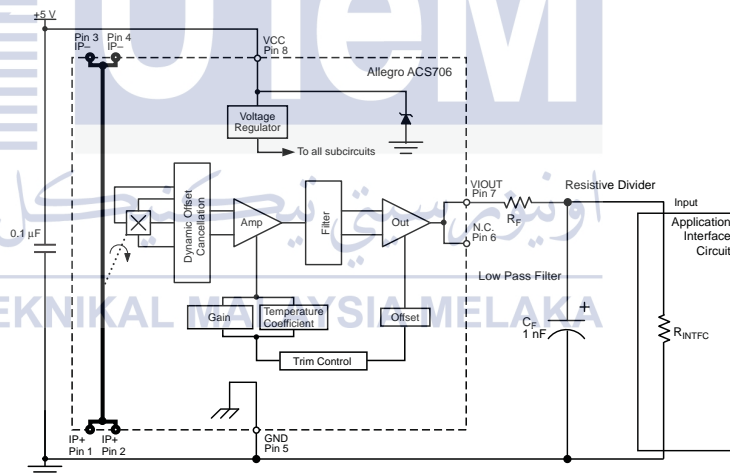
Application 7. Using the FILTER pin provided on the ACS712 eliminates the attenuation effects of the resistor divider between R_F and R_{INTFC}, shown in Application 6.

Allegro MicroSystems, LLC
115 Northeast Cutoff
Worcester, Massachusetts 01615-0036 U.S.A.
1.508.853.5000; www.allegromicro.com

13

ACS712

Fully Integrated, Hall Effect-Based Linear Current Sensor IC with 2.1 kVRMS Isolation and a Low-Resistance Current Conductor

Package LC, 8-pin SOIC

4.90 ±0.10

8

3.90 ±0.10

6.00 ±0.20

1   2

8°
0°

0.25
0.17

1.04 REF

1.27
0.40

0.25 BSC

SEATING PLANE
GAUGE PLANE

0.65

8

1.27

1.75

5.60

1   2

C PCB Layout Reference View

8X

⌓ 0.10 C

Branded Face

C

SEATING
PLANE

1.75 MAX

0.51
0.31

0.25
0.10

1.27 BSC

NNNNNNN
TPP-AAA
LLLLL

1

B Standard Branding Reference View

N = Device part number
T = Device temperature range
P = Package Designator
A = Amperage
L = Lot number
Belly Brand = Country of Origin

For Reference Only; not for tooling use (reference MS-012AA)
Dimensions in millimeters
Dimensions exclusive of mold flash, gate burrs, and dambar protrusions
Exact case and lead configuration at supplier discretion within limits shown

A Terminal #1 mark area

B Branding scale and appearance at supplier discretion

C Reference land pattern layout (reference IPC7351)

D SOIC127P600X175-8M); all pads a minimum of 0.20 mm from all
adjacent pads; adjust as necessary to meet application process
requirements and PCB layout tolerances

Allegro MicroSystems, LLC
115 Northeast Cutoff
Worcester, Massachusetts 01615-0036 U.S.A.
1.508.853.5000; www.allegromicro.com

14

Allegro
MicroSystems, LLC

ACS712

Fully Integrated, Hall Effect-Based Linear Current Sensor IC with 2.1 kVRMS Isolation and a Low-Resistance Current Conductor

Revision History

Revision	Revision Date	Description of Revision
Rev. 15	November 16, 2012	Update rise time and isolation, I_{OUT} reference data, patents

For the latest version of this document, visit our website:

www.allegromicro.com

Allegro MicroSystems, LLC
115 Northeast Cutoff
Worcester, Massachusetts 01615-0036 U.S.A.
1.508.853.5000; www.allegromicro.com

15

Power MOSFET

PRODUCT SUMMARY

V_{DS} (V)	- 100	
$R_{DS(on)}$ (Ω)	V_{GS} = - 10 V	0.20
Q_g (Max.) (nC)	61	
Q_{gs} (nC)	14	
Q_{gd} (nC)	29	
Configuration	Single	

TO-220AB

P-Channel MOSFET
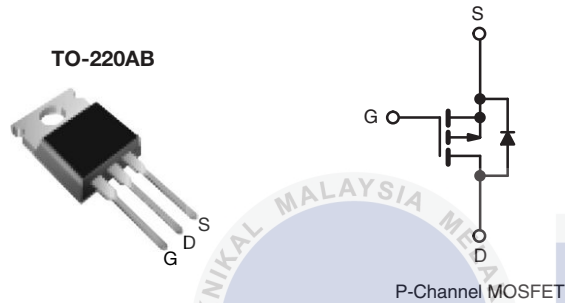
FEATURES
- Dynamic dV/dt Rating
- Repetitive Avalanche Rated
- P-Channel
- 175 °C Operating Temperature
- Fast Switching
- Ease of Paralleling
- Simple Drive Requirements
- Compliant to RoHS Directive 2002/95/EC

Available

RoHS*
COMPLIANT

DESCRIPTION

Third generation Power MOSFETs from Vishay provide the designer with the best combination of fast switching, ruggedized device design, low on-resistance and cost-effectiveness.

The TO-220AB package is universally preferred for all commercial-industrial applications at power dissipation levels to approximately 50 W. The low thermal resistance and low package cost of the TO-220AB contribute to its wide acceptance throughout the industry.

ORDERING INFORMATION

Package	TO-220AB
Lead (Pb)-free	IRF9540PbF
	SiHF9540-E3
SnPb	IRF9540
	SiHF9540
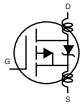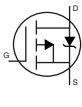
ABSOLUTE MAXIMUM RATINGS (T_C = 25 °C, unless otherwise noted)

PARAMETER			SYMBOL	LIMIT	UNIT
Drain-Source Voltage			V_{DS}	- 100	V
Gate-Source Voltage			V_{GS}	± 20	
Continuous Drain Current	V_{GS} at - 10 V	T_C = 25 °C	I_D	- 19	A
		T_C = 100 °C		- 13	
Pulsed Drain Current[a]			I_{DM}	- 72	
Linear Derating Factor				1.0	W/°C
Single Pulse Avalanche Energy[b]			E_{AS}	640	mJ
Repetitive Avalanche Current[a]			I_{AR}	- 19	A
Repetitive Avalanche Energy[a]			E_{AR}	15	mJ
Maximum Power Dissipation	T_C = 25 °C		P_D	150	W
Peak Diode Recovery dV/dt[c]			dV/dt	- 5.5	V/ns
Operating Junction and Storage Temperature Range			T_J, T_{stg}	- 55 to + 175	°C
Soldering Recommendations (Peak Temperature)	for 10 s			300[d]	
Mounting Torque	6-32 or M3 screw			10	lbf · in
				1.1	N · m

Notes
a. Repetitive rating; pulse width limited by maximum junction temperature (see fig. 11).
b. V_{DD} = - 25 V, starting T_J = 25 °C, L = 2.7 mH, R_g = 25 Ω, I_{AS} = - 19 A (see fig. 12).
c. I_{SD} ≤ - 19 A, dI/dt ≤ 200 A/µs, V_{DD} ≤ V_{DS}, T_J ≤ 175 °C.
d. 1.6 mm from case.

* Pb containing terminations are not RoHS compliant, exemptions may apply

This datasheet is subject to change without notice.
THE PRODUCT DESCRIBED HEREIN AND THIS DATASHEET ARE SUBJECT TO SPECIFIC DISCLAIMERS, SET FORTH AT www.vishay.com/doc?91000

THERMAL RESISTANCE RATINGS

PARAMETER	SYMBOL	TYP.	MAX.	UNIT
Maximum Junction-to-Ambient	R_{thJA}	-	62	
Case-to-Sink, Flat, Greased Surface	R_{thCS}	0.50	-	°C/W
Maximum Junction-to-Case (Drain)	R_{thJC}	-	1.0	

SPECIFICATIONS (T_J = 25 °C, unless otherwise noted)

PARAMETER	SYMBOL	TEST CONDITIONS		MIN.	TYP.	MAX.	UNIT
Static							
Drain-Source Breakdown Voltage	V_{DS}	V_{GS} = 0 V, I_D = - 250 µA		- 100	-	-	V
V_{DS} Temperature Coefficient	$\Delta V_{DS}/T_J$	Reference to 25 °C, I_D = - 1 mA		-	- 0.087	-	V/°C
Gate-Source Threshold Voltage	$V_{GS(th)}$	V_{DS} = V_{GS}, I_D = - 250 µA		- 2.0	-	- 4.0	V
Gate-Source Leakage	I_{GSS}	V_{GS} = ± 20 V		-	-	± 100	nA
Zero Gate Voltage Drain Current	I_{DSS}	V_{DS} = - 100 V, V_{GS} = 0 V		-	-	- 100	µA
		V_{DS} = - 80 V, V_{GS} = 0 V, T_J = 150 °C		-	-	- 500	
Drain-Source On-State Resistance	$R_{DS(on)}$	V_{GS} = - 10 V	I_D = - 11 A[b]	-	-	0.20	Ω
Forward Transconductance	g_{fs}	V_{DS} = - 50 V, I_D = - 11 A[b]		6.2	-	-	S
Dynamic							
Input Capacitance	C_{iss}	V_{GS} = 0 V, V_{DS} = - 25 V, f = 1.0 MHz, see fig. 5		-	1400	-	pF
Output Capacitance	C_{oss}			-	590	-	
Reverse Transfer Capacitance	C_{rss}			-	140	-	
Total Gate Charge	Q_g	V_{GS} = - 10 V	I_D = - 19 A, V_{DS} = - 80 V, see fig. 6 and 13[b]	-	-	61	nC
Gate-Source Charge	Q_{gs}			-	-	14	
Gate-Drain Charge	Q_{gd}			-	-	29	
Turn-On Delay Time	$t_{d(on)}$	V_{DD} = - 50 V, I_D = - 19 A, R_g = 9.1 Ω, R_D = 2.4 Ω, see fig. 10[b]		-	16	-	ns
Rise Time	t_r			-	73	-	
Turn-Off Delay Time	$t_{d(off)}$			-	34	-	
Fall Time	t_f			-	57	-	
Internal Drain Inductance	L_D	Between lead, 6 mm (0.25") from package and center of die contact		-	4.5	-	nH
Internal Source Inductance	L_S			-	7.5	-	
Drain-Source Body Diode Characteristics							
Continuous Source-Drain Diode Current	I_S	MOSFET symbol showing the integral reverse p - n junction diode		-	-	- 19	A
Pulsed Diode Forward Current[a]	I_{SM}			-	-	- 72	
Body Diode Voltage	V_{SD}	T_J = 25 °C, I_S = - 19 A, V_{GS} = 0 V[b]		-	-	- 5.0	V
Body Diode Reverse Recovery Time	t_{rr}	T_J = 25 °C, I_F = - 19 A, dI/dt = 100 A/µs[b]		-	130	260	ns
Body Diode Reverse Recovery Charge	Q_{rr}			-	0.35	0.70	µC
Forward Turn-On Time	t_{on}	Intrinsic turn-on time is negligible (turn-on is dominated by L_S and L_D)					

Notes
a. Repetitive rating; pulse width limited by maximum junction temperature (see fig. 11).
b. Pulse width ≤ 300 µs; duty cycle ≤ 2 %.
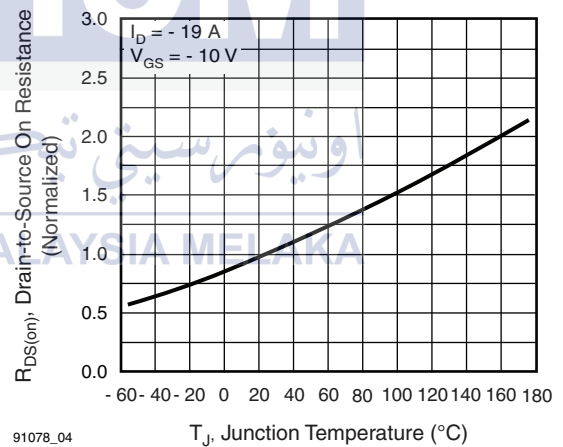
TYPICAL CHARACTERISTICS (25 °C, unless otherwise noted)

91078_01

- V$_{DS}$, Drain-to-Source Voltage (V)
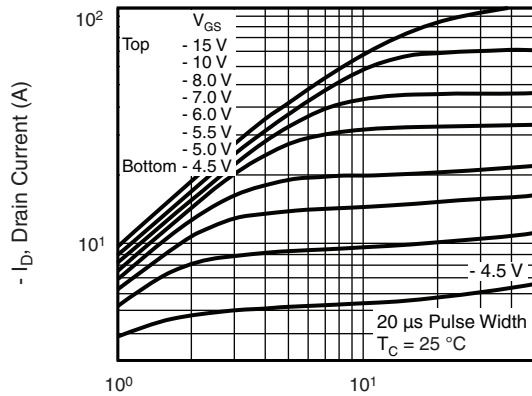
Fig. 1 - Typical Output Characteristics, T$_C$ = 25 °C

91078_03
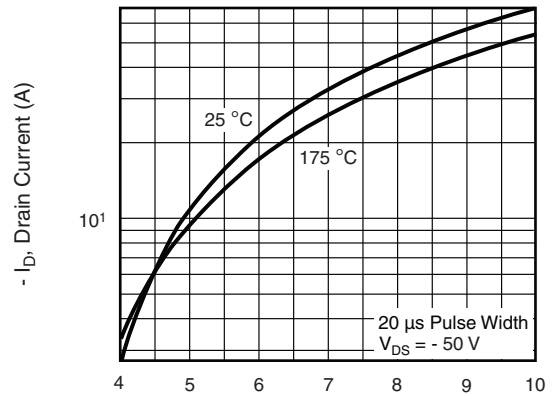
- V$_{GS}$, Gate-to-Source Voltage (V)

Fig. 3 - Typical Transfer Characteristics

91078_02

- V$_{DS}$, Drain-to-Source Voltage (V)
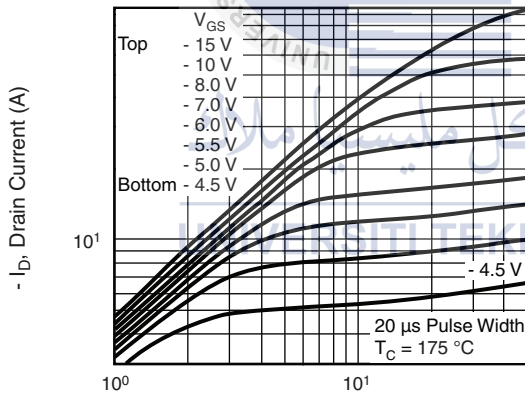
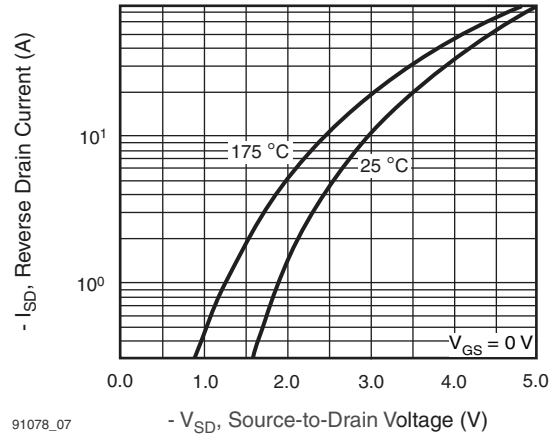**Fig. 2 - Typical Output Characteristics, T$_C$ = 175 ° C**

91078_04

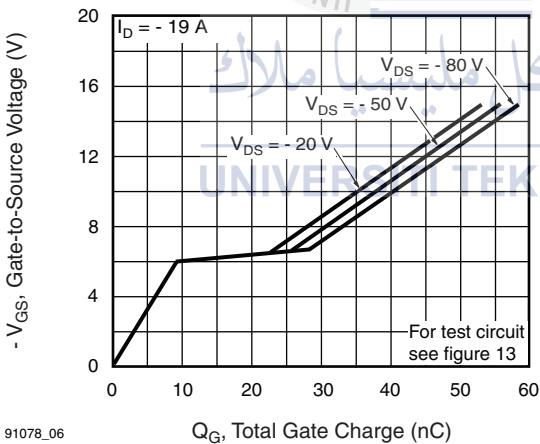T$_J$, Junction Temperature (°C)

Fig. 4 - Normalized On-Resistance vs. Temperature
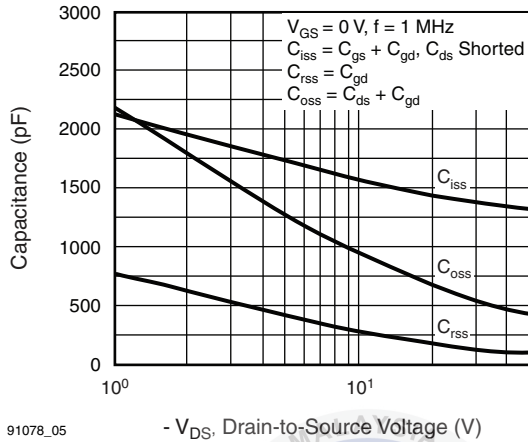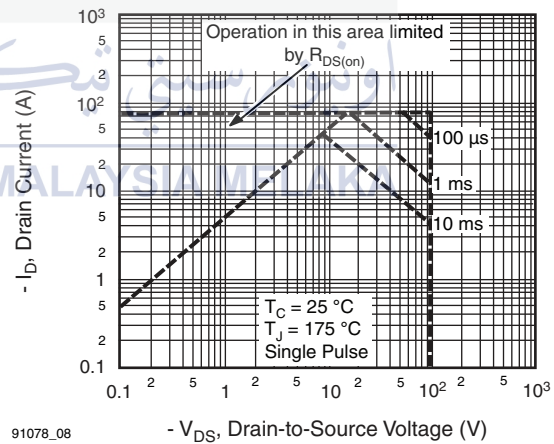
Fig. 5 - Typical Capacitance vs. Drain-to-Source Voltage
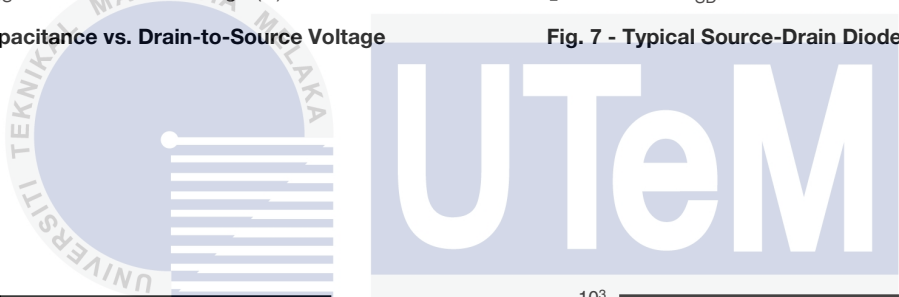

Fig. 7 - Typical Source-Drain Diode Forward Voltage

Fig. 6 - Typical Gate Charge vs. Gate-to-Source Voltage

Fig. 8 - Maximum Safe Operating Area

Fig. 10a - Switching Time Test Circuit
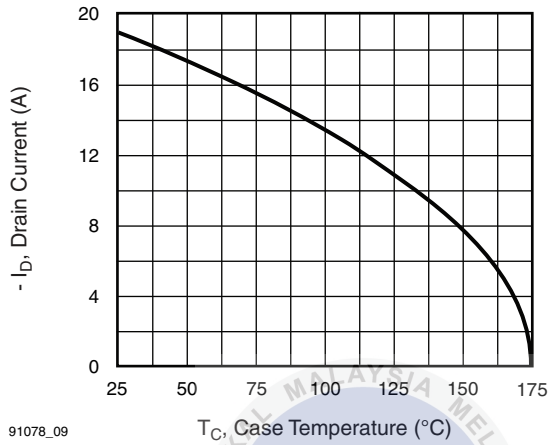
Fig. 9 - Maximum Drain Current vs. Case Temperature
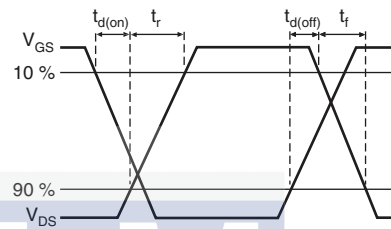
Fig. 10b - Switching Time Waveforms

Notes:
1. Duty Factor, D = t_1/t_2
2. Peak T_j = P_{DM} x Z_{thJC} + T_C
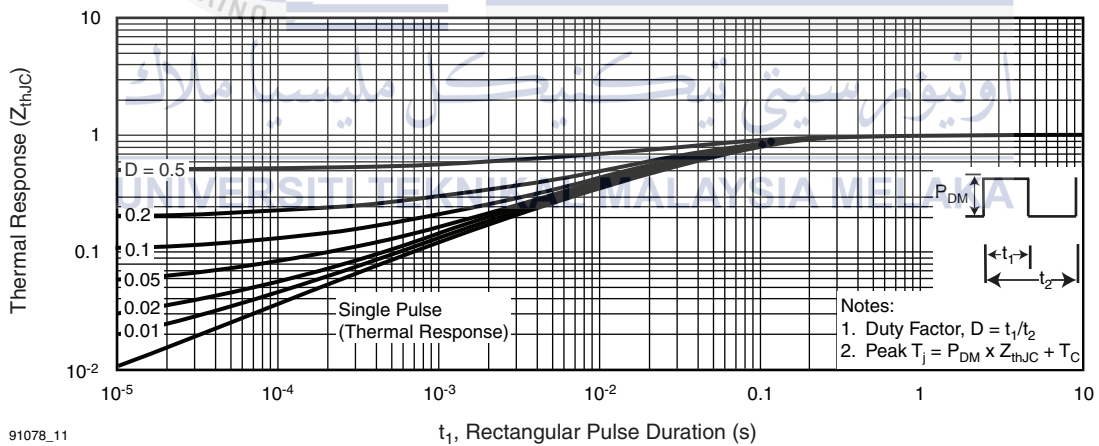
Fig. 11 - Maximum Effective Transient Thermal Impedance, Junction-to-Case
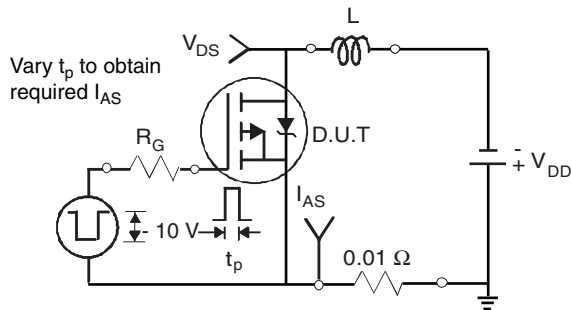
IRF9540, SiHF9540

Vishay Siliconix

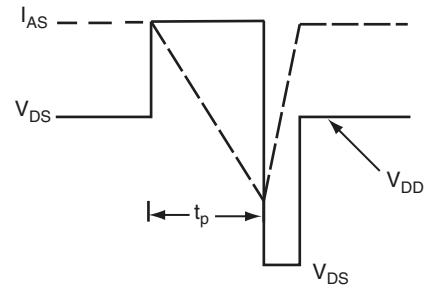Fig. 12a - Unclamped Inductive Test Circuit

Fig. 12b - Unclamped Inductive Waveforms
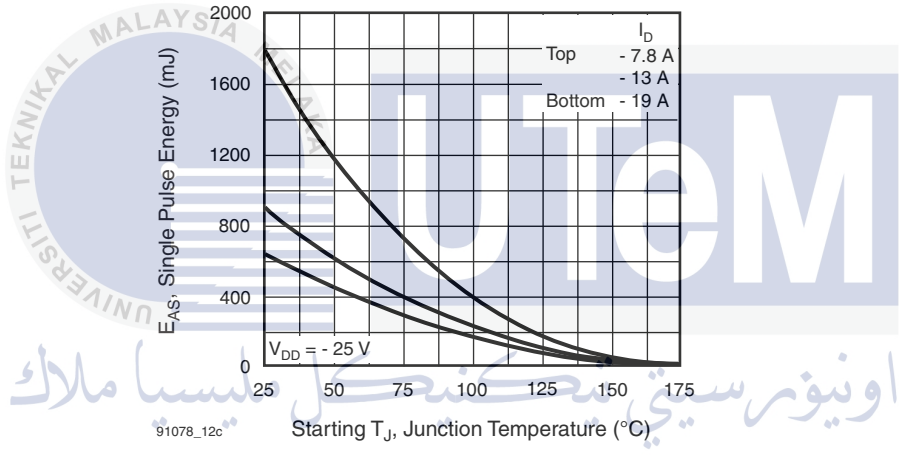
Fig. 12c - Maximum Avalanche Energy vs. Drain Current
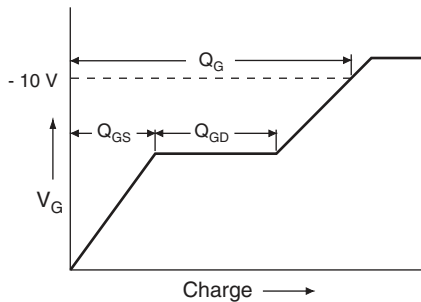
Fig. 13a - Basic Gate Charge Waveform
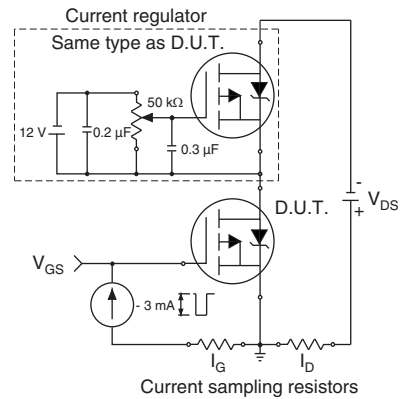
Fig. 13b - Gate Charge Test Circuit

Peak Diode Recovery dV/dt Test Circuit

Circuit layout considerations
- Low stray inductance
- Ground plane
- Low leakage inductance current transformer

- dV/dt controlled by R_g
- I_{SD} controlled by duty factor "D"
- D.U.T. - device under test
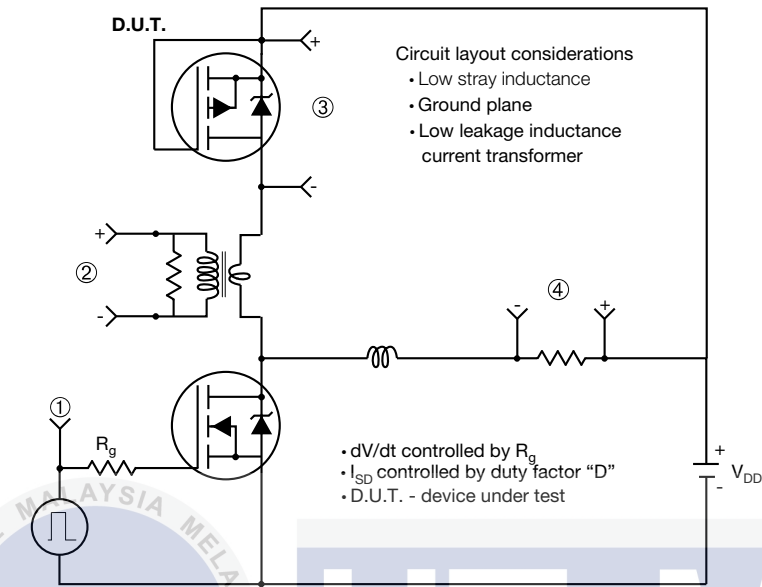
Note
- Compliment N-Channel of D.U.T. for driver

① Driver gate drive

$$D = \frac{P.W.}{Period}$$

$V_{GS} = - 10\ V^a$

② D.U.T. I_{SD} waveform

Reverse recovery current

Body diode forward current

dI/dt

③ D.U.T. V_{DS} waveform

Diode recovery dV/dt

V_{DD}

Re-applied voltage

Body diode forward drop

④ Inductor current

Ripple ≤ 5 %

I_{SD}
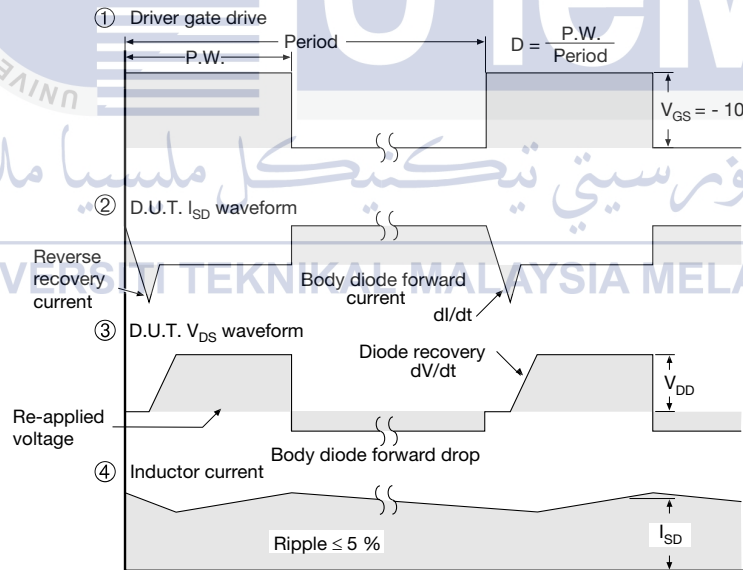
Note
a. $V_{GS} = - 5\ V$ for logic level and - 3 V drive devices

Fig. 14 - For P-Channel

TO-220AB
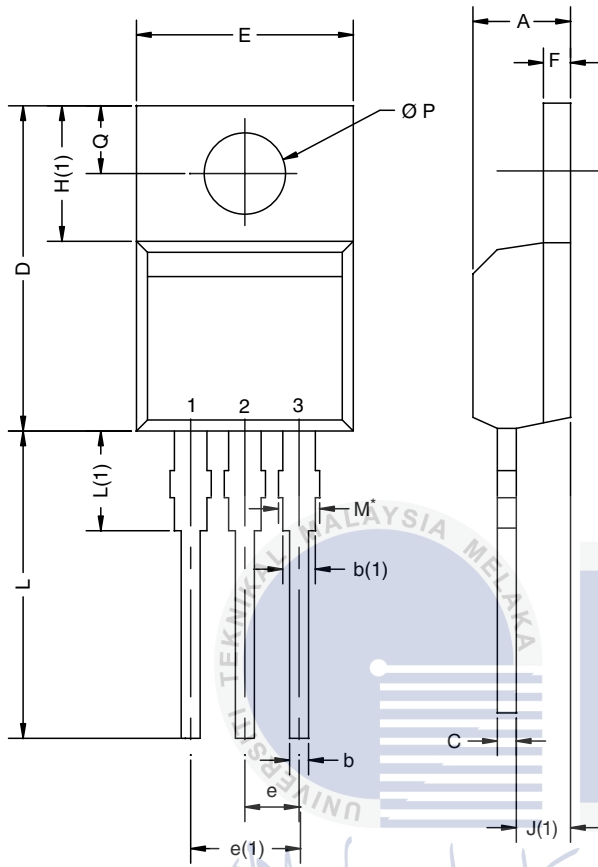
DIM.	MILLIMETERS		INCHES	
	MIN.	MAX.	MIN.	MAX.
A	4.25	4.65	0.167	0.183
b	0.69	1.01	0.027	0.040
b(1)	1.20	1.73	0.047	0.068
c	0.36	0.61	0.014	0.024
D	14.85	15.49	0.585	0.610
E	10.04	10.51	0.395	0.414
e	2.41	2.67	0.095	0.105
e(1)	4.88	5.28	0.192	0.208
F	1.14	1.40	0.045	0.055
H(1)	6.09	6.48	0.240	0.255
J(1)	2.41	2.92	0.095	0.115
L	13.35	14.02	0.526	0.552
L(1)	3.32	3.82	0.131	0.150
Ø P	3.54	3.94	0.139	0.155
Q	2.60	3.00	0.102	0.118

ECN: T13-0724-Rev. O, 14-Oct-13
DWG: 5471

Note

* M = 1.32 mm to 1.62 mm (dimension including protrusion)
Heatsink hole for HVM

For technical questions, contact: hvm@vishay.com

Disclaimer

ALL PRODUCT, PRODUCT SPECIFICATIONS AND DATA ARE SUBJECT TO CHANGE WITHOUT NOTICE TO IMPROVE RELIABILITY, FUNCTION OR DESIGN OR OTHERWISE.

Vishay Intertechnology, Inc., its affiliates, agents, and employees, and all persons acting on its or their behalf (collectively, "Vishay"), disclaim any and all liability for any errors, inaccuracies or incompleteness contained in any datasheet or in any other disclosure relating to any product.

Vishay makes no warranty, representation or guarantee regarding the suitability of the products for any particular purpose or the continuing production of any product. To the maximum extent permitted by applicable law, Vishay disclaims (i) any and all liability arising out of the application or use of any product, (ii) any and all liability, including without limitation special, consequential or incidental damages, and (iii) any and all implied warranties, including warranties of fitness for particular purpose, non-infringement and merchantability.

Statements regarding the suitability of products for certain types of applications are based on Vishay's knowledge of typical requirements that are often placed on Vishay products in generic applications. Such statements are not binding statements about the suitability of products for a particular application. It is the customer's responsibility to validate that a particular product with the properties described in the product specification is suitable for use in a particular application. Parameters provided in datasheets and/or specifications may vary in different applications and performance may vary over time. All operating parameters, including typical parameters, must be validated for each customer application by the customer's technical experts. Product specifications do not expand or otherwise modify Vishay's terms and conditions of purchase, including but not limited to the warranty expressed therein.

Except as expressly indicated in writing, Vishay products are not designed for use in medical, life-saving, or life-sustaining applications or for any other application in which the failure of the Vishay product could result in personal injury or death. Customers using or selling Vishay products not expressly indicated for use in such applications do so at their own risk. Please contact authorized Vishay personnel to obtain written terms and conditions regarding products designed for such applications.

No license, express or implied, by estoppel or otherwise, to any intellectual property rights is granted by this document or by any conduct of Vishay. Product names and markings noted herein may be trademarks of their respective owners.

Material Category Policy

Vishay Intertechnology, Inc. hereby certifies that all its products that are identified as RoHS-Compliant fulfill the definitions and restrictions defined under Directive 2011/65/EU of The European Parliament and of the Council of June 8, 2011 on the restriction of the use of certain hazardous substances in electrical and electronic equipment (EEE) - recast, unless otherwise specified as non-compliant.

Please note that some Vishay documentation may still make reference to RoHS Directive 2002/95/EC. We confirm that all the products identified as being compliant to Directive 2002/95/EC conform to Directive 2011/65/EU.

Vishay Intertechnology, Inc. hereby certifies that all its products that are identified as Halogen-Free follow Halogen-Free requirements as per JEDEC JS709A standards. Please note that some Vishay documentation may still make reference to the IEC 61249-2-21 definition. We confirm that all the products identified as being compliant to IEC 61249-2-21 conform to JEDEC JS709A standards.

FAIRCHILD

SEMICONDUCTOR ™

Discrete POWER & Signal Technologies

BC548
BC548A
BC548B
BC548C

E **B** **C** **TO-92**
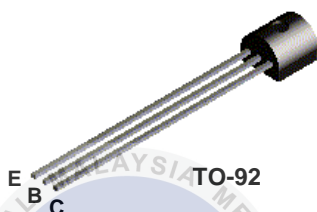
NPN General Purpose Amplifier

This device is designed for use as general purpose amplifiers and switches requiring collector currents to 300 mA. Sourced from Process 10. See PN100A for characteristics.

Absolute Maximum Ratings*

TA = 25°C unless otherwise noted

Symbol	Parameter	Value	Units
V_{CEO}	Collector-Emitter Voltage	30	V
V_{CES}	Collector-Base Voltage	30	V
V_{EBO}	Emitter-Base Voltage	5.0	V
I_C	Collector Current - Continuous	500	mA
T_J, T_{stg}	Operating and Storage Junction Temperature Range	-55 to +150	°C

*These ratings are limiting values above which the serviceability of any semiconductor device may be impaired.

NOTES:
1) These ratings are based on a maximum junction temperature of 150 degrees C.
2) These are steady state limits. The factory should be consulted on applications involving pulsed or low duty cycle operations.

Thermal Characteristics

TA = 25°C unless otherwise noted

Symbol	Characteristic	Max	Units
		BC548 / A / B / C	
P_D	Total Device Dissipation	625	mW
	Derate above 25°C	5.0	mW/°C
$R_{\theta JC}$	Thermal Resistance, Junction to Case	83.3	°C/W
$R_{\theta JA}$	Thermal Resistance, Junction to Ambient	200	°C/W

NPN General Purpose Amplifier

(continued)

Electrical Characteristics   TA = 25°C unless otherwise noted

Symbol	Parameter	Test Conditions		Min	Max	Units

OFF CHARACTERISTICS

Symbol	Parameter	Test Conditions		Min	Max	Units
$V_{(BR)CEO}$	Collector-Emitter Breakdown Voltage	$I_C = 10$ mA, $I_B = 0$		30		V
$V_{(BR)CBO}$	Collector-Base Breakdown Voltage	$I_C = 10$ µA, $I_E = 0$		30		V
$V_{(BR)CES}$	Collector-Base Breakdown Voltage	$I_C = 10$ µA, $I_E = 0$		30		V
$V_{(BR)EBO}$	Emitter-Base Breakdown Voltage	$I_E = 10$ µA, $I_C = 0$		5.0		V
I_{CBO}	Collector Cutoff Current	$V_{CB} = 30$ V, $I_E = 0$			15	nA
		$V_{CB} = 30$ V, $I_E = 0$, $T_A = +150$ °C			5.0	µA

ON CHARACTERISTICS

Symbol	Parameter	Test Conditions		Min	Max	Units
h_{FE}	DC Current Gain	$V_{CE} = 5.0$ V, $I_C = 2.0$ mA	**548**	110	800	
			548A	110	220	
			548B	200	450	
			548C	420	800	
$V_{CE(sat)}$	Collector-Emitter Saturation Voltage	$I_C = 10$ mA, $I_B = 0.5$ mA			0.25	V
		$I_C = 100$ mA, $I_B = 5.0$ mA			0.60	V
$V_{BE(on)}$	Base-Emitter On Voltage	$V_{CE} = 5.0$ V, $I_C = 2.0$ mA		0.58	0.70	V
		$V_{CE} = 5.0$ V, $I_C = 10$ mA			0.77	V

SMALL SIGNAL CHARACTERISTICS

Symbol	Parameter	Test Conditions		Min	Max	Units
h_{fe}	Small-Signal Current Gain	$I_C = 2.0$ mA, $V_{CE} = 5.0$ V, f = 1.0 kHz		125	900	
NF	Noise Figure	$V_{CE} = 5.0$ V, $I_C = 200$ µA, $R_S = 2.0$ kΩ, f = 1.0 kHz, $B_W = 200$ Hz			10	dB